HHS Public Access

Author manuscript

Nat Genet. Author manuscript; available in PMC 2020 October 27.

Published in final edited form as:

Nat Genet. 2020 May ; 52(5): 494–504. doi:10.1038/s41588-020-0611-8.

Genome-wide association meta-analyses combining multiple risk phenotypes provides insights into the genetic architecture of cutaneous melanoma susceptibility

A full list of authors and affiliations appears at the end of the article.

Abstract

Most genetic susceptibility to cutaneous melanoma remains to be discovered. Meta-analysis genome-wide association study (GWAS) of 36,760 melanoma cases (67% newly-genotyped) and 375,188 controls identified 54 significant loci with 68 independent SNPs. Analysis of risk estimates across geographical regions and host factors suggests the acral melanoma subtype is uniquely unrelated to pigmentation. Combining this meta-analysis with nevus count and hair color GWAS, and transcriptome association approaches, uncovered 31 potential secondary loci, for a total of 85 cutaneous melanoma susceptibility loci. These findings provide substantial insights into cutaneous melanoma genetic architecture, reinforcing the importance of nevogenesis, pigmentation, and telomere maintenance together with identifying potential new pathways for cutaneous melanoma pathogenesis.

Cutaneous melanoma is a deadly malignancy with increasing incidence and burden in fair-skinned populations worldwide[1]. Increased risk for cutaneous melanoma is caused by high exposure to ultraviolet radiation[2], as well as host factors including family history[3,4], pigmentary phenotypes[5], number of melanocytic nevi[6,7], longer telomeres[8,9], and immunosuppression[10].

Identified melanoma genetic risk variants include rare, highly penetrant mutations in genes such as *CDKN2A*[11,12] and *POT1*[13,14], as well as more common variants (e.g., lower-

@Corresponding authors: Mark M. Iles (M.M.Iles@leeds.ac.uk), Matthew H. Law (Matthew.Law@qimrberghofer.edu.au), Maria Teresa Landi (landim@mail.nih.gov).

*Jointly supervised this work

#Contributed equally

Author Contributions

MTL, MMI, MHL- Project conceptualization and design

DTB, SM, MTL, SJC - Funding support

MTL, DTB, SM, MJM, SJ, MMI, MHL - Results interpretation and study supervision

MJM, MTL, MMI, KB, JC, MHL - Manuscript writing

JS, MMI, KB, TZ, JC, DLD, MHL - Data analyses

AJS, PG, SP, EN - Study coordination and data collection

MTL, DTB, SM, MJM, AJS, PG, MB, DC, JC, MCF, TZ, MR, AJT, CM, JM, AH, LS, IS, RS, RY, AMG, MP, KPK, LP, PQ, CP, LC, MZ, PG2, AR, LE, SM2, LR, BHS, MAL, LDR, DM, MM, KK, LAA, CIA, PAA, MA, EA, HPS, VB, BD, LMB, KPB, WVC, VC, JEC, TD, MF, SF, EF, SS, PG3, ZG, EMG, SG, AG, NAG, JH2, MH, JH3, PH, AH2, MH2, VH, DH, CI, RK, JL, GML, JEL, XL, JL2, RMM, MM2, JM2, KM, HM, AM, EKM, REN, SN, DRN, HO, NO, LGF, JAP, AAQ, GLR, JR, CR, CR2, NJS, MS, DS, HS, LAS, MS2, FS, AJS2, NVDS, NAK, AV, LW, SVW, LW2, RAS, AH3, KJ, MM3, AV2, WZ, KAP, DEE, JH, BH, NKH, PAK, CB, GWM, CMO, CH, AMD, NGM, EE, GJM, GL, PDPP, DFE, JHB, AEC, GA, DLD, DCW, HG, ADN, MAT, JANB, KP, SJC, KMB, FD, SP, EN, JS, MMI, MHL - Participated in data collection, results interpretation and manuscript review

penetrance variants in *MC1R*)[15,16]. Genome-wide association studies (GWAS) of cutaneous melanoma susceptibility in populations of European ancestry have identified 21 genetic loci reaching genome-wide significance ($P < 5 \times 10^{-8}$)[17-24]. Additional approaches, including family-based analyses of cutaneous melanoma[25,26], combining cutaneous melanoma and nevus count GWAS[27] and transcriptome-wide association studies (TWAS)[28] have identified further loci that, despite not containing SNPs reaching $P < 5 \times 10^{-8}$ in a cutaneous melanoma-only GWAS, most likely influence melanoma risk.

This meta-analysis of cutaneous melanoma susceptibility is more than three times the effective sample size of previous cutaneous melanoma GWAS, providing unprecedented power to identify cutaneous melanoma susceptibility variants and enhanced distinction of independent variants in known cutaneous melanoma susceptibility regions. We report here 68 independent cutaneous melanoma associated variants across 54 loci that confirm the importance of key functional pathways and highlight previously unknown cutaneous melanoma etiologic routes (Tables 1-2). Stratified analyses showed a lack of involvement of the pigmentation pathway for acral melanoma, in line with observational data[29]. The combined analysis of cutaneous melanoma, nevus and hair color GWAS data, and use of expression data through TWAS, identified 31 secondary, potential loci.

Results

Study overview

We performed a GWAS meta-analysis of cutaneous melanoma susceptibility with 30,134 clinically-confirmed cutaneous melanoma cases (Online Methods), 6,626 self-reported cutaneous melanoma cases and 375,188 cutaneous melanoma -free controls from the United Kingdom, United States, Australia, Northern and Western Europe as well as the Mediterranean – a highly sun exposed population often under-represented in cutaneous melanoma studies (Supplementary Table 1). Of these, 24,756 cases (67%) and 358,734 controls (96%) had not been included in any previous melanoma GWAS.

Separately, we performed total (clinically confirmed cases + self-reported cases from 23andMe, Inc. and a subset of UK Biobank cases with only self-reported cutaneous melanoma status) and confirmed-only cutaneous melanoma meta-analyses to determine the power gained by including self-reported cutaneous melanoma cases. Risk loci were deemed genome-wide significant when variants had fixed effects meta-analysis P-values $< 5 \times 10^{-8}$ (P_{meta}); where variants exhibited notable heterogeneity ($I^2 > 31\%$)[30] random effects P-values (P_{meta_r}) were also required to be $< 5 \times 10^{-8}$ (Online Methods). Q-Q plots (Supplementary Figure 1) and linkage disequilibrium score regression[31] (LDSC; Online Methods) intercepts showed minimal inflation for individual studies (mostly < 1.04; Supplementary Table 1), indicating adequate control of population stratification.

Before including the self-report GWAS data, we used LDSC[31] to verify their genetic correlation (Rg) with the confirmed-only GWAS meta-analysis (Supplementary Note; Supplementary Table 2). Based on the high Rg and similarity in h^2 estimates for self-report and clinically confirmed cutaneous melanoma cases (Supplementary Note), we performed an overall total cutaneous melanoma meta-analysis (h^2_{total}= 0.11, 95% CI = 0.08–0.15). The

lambda and LDSC intercept for the total cutaneous melanoma meta-analysis indicated that the majority of inflation is due to polygenic signal ($\lambda = 1.165$, intercept = 1.054, ratio = 0.17; Supplementary Table 2). A similar h^2_{total} (12%) was estimated using genetic effect-size distribution inference from summary level data (GENESIS; Online Methods)[32].

Conditional and joint analysis of the total cutaneous melanoma meta-analysis summary statistics using GCTA[33] identified a total of 54 loci meeting our requirements for genome-wide significance (Online Methods; Figure 1, Extended Data Figure 1-2). Results for loci previously reported by cutaneous melanoma GWAS reaching significance in the total meta-analysis are presented in Table 1. Results for loci not previously reported by a cutaneous melanoma GWAS are summarized in Table 2. In addition to the 54 lead variants, 14 independent variants with linkage disequilibrium (LD) $r^2_{EUR} < 0.05$ with lead variants at or near 6 loci (*TERT*, *AGR3*, *CDKN2A*, *OCA2*, *MC1R*, and *TP53*) were identified (Supplementary Table 3). Individual regional association plots for the association signals have been provided as Supplementary Data 1. Conditional and joint analysis of summary data identified a further 9 variants at or near *SLC45A2*, *IRF4*, *AGR3*, *CCND1*, *GPRC5A*, *FTO,* and *MC1R*; however, these additional variants were not carried forward, having either $P_{meta} > 5 \times 10^{-8}$ in the single variant analysis or excess heterogeneity ($I^2 > 31\%$) and $P_{meta\_r} < 5 \times 10^{-8}$ (Supplementary Table 4). In addition, we used GENESIS (Online Methods), which enables a reformulation of the variance explained by associated SNPs to estimate a theoretical optimal area under the curve (AUC), rather than formally testing this using a training and prediction set[32] to estimate the potential AUC. The estimated AUC was 66.8%, compared to ~64% in the 2015 cutaneous melanoma meta-analysis[23]. This estimate does not include any host factors and would require benchmarking in a prospective study for validation.

Previous cutaneous melanoma GWAS have identified 21 genome-wide significant loci[17-24]. Family-based methods or the combination of cutaneous melanoma with nevus count have identified a further 12 loci including *IRF4*, *MITF, HDAC4,* and *GPRC5A*[25-27]. The lead SNPs from many of these loci are associated with pigmentation, tanning response, nevus count, and telomere maintenance (Supplementary Table 5). Other SNPs are proximal to DNA repair genes. Some loci are associated with more than one trait (Tables 1-2). Our analysis confirms 19 of the 21 loci previously reaching genome-wide significance (Table 1; Supplementary Note). The total cutaneous melanoma meta-analysis also confirms the previously reported *IRF4* and *MITF* associations[25-27,34,35], as well as 6 regions previously identified only by combining nevus count and cutaneous melanoma GWAS data[27] (Table 2; Supplementary Note). These results demonstrate the ability of cross-trait GWAS to identify disease loci. The remaining 27 loci have not previously been reported as cutaneous melanoma susceptibility loci (Table 2; Supplementary Table 3). The results for the pathologically confirmed-only cutaneous melanoma cases (N = 30,134; Supplementary Table 1) are reported in the Supplementary Note, Extended Data Figure 2-3, Supplementary Table 6. Our full meta-analysis identified 11 loci not found in the confirmed-only GWAS meta-analysis, demonstrating the advantage of including the 6,626 self-reported cutaneous melanoma cases and over 290,000 controls (Supplementary Table 1). Results for SNPs with a fixed or random $P < 5 \times 10^{-7}$, from the total meta-analysis are reported in Supplementary Table 7.

Melanoma associations by sex, age at diagnosis and subtype

We performed separate GWAS by sex, age at cutaneous melanoma diagnosis (≤40, 40–60, ≥60 years) and major cutaneous melanoma subtypes (superficial spreading (SS), lentigo maligna (LM), nodular melanoma (NM), and acral lentiginous (AL)) to identify variants associated with select subgroups (Supplementary Table 8). Our analysis identified no additional variants after adjustment for multiple testing ($5 \times 10^{-8}/9$), suggesting that if such variants exist they are undetectable at our current sample size.

We also performed polygenic risk score (PRS) analyses based on the lead independent genome-wide significant SNPs for nevus count (10 variants; Online Methods) and hair color (276 variants; Online Methods) to explore further whether either trait's association with cutaneous melanoma differs across phenotypic subtypes (significance threshold = 0.05/28; Online Methods). We observed no significant differences in the distribution of the tested PRSs by sex or age at cutaneous melanoma diagnosis. We did, however, detect differences in the distribution of the hair color PRS for the acral lentiginous subtype compared to all non-acral subtypes ($P = 2.1 \times 10^{-4}$). Our analyses indicated that genetically-predicted pigmentation in acral lentiginous cases was no different to controls (P = 0.65, Extended Data Figure 4) and darker than in superficial spreading, lentigo maligna and nodular melanoma cases ($P = 5.3 \times 10^{-5}$, 0.01, 4.8×10^{-4}, respectively). These findings provide strong genetic evidence that the pigmentation pathway is far less important for risk of acral lentiginous melanoma than for other subtypes of cutaneous melanoma. No significant differences were observed by subtype for the nevus count PRS.

Variant annotation with cutaneous melanoma risk phenotypes

To investigate possible biological pathways underlying cutaneous melanoma signals, variants independently associated with cutaneous melanoma in the total meta-analysis were evaluated in GWAS of telomere length, tanning response, pigmentation and nevus count (Online Methods, Table 1 and 2, Supplementary Tables 5,7-8). Using a Bonferroni-corrected threshold of phenotype P-value < 0.00074 (0.05/68 independent SNPs), 18 of the 35 novel loci are associated with tanning response or pigmentation (Table 2, Supplementary Table 5), further indicating the importance of pigmentation pathways in cutaneous melanoma susceptibility. Several new loci, including rs12473635 near *DTNB* and rs78378222 near *TP53,* are associated with nevus count, reinforcing the role of nevi in cutaneous melanoma susceptibility. Furthermore, four novel loci have previously been associated with telomere length (rs3950296/*TERC*, rs4731207/*POT1*, rs2967383/*MPHOSPH6*, and rs143190905/*RTEL1*[36]) (Table 2, Supplementary Table 5) providing additional support for the role of telomere maintenance in cutaneous melanoma susceptibility following earlier findings that genetic determinants of telomere length are generally associated with melanoma risk[13,14,37]. Other newly-discovered lead variants are not associated with these phenotypes, suggesting novel pathways.

Additional approaches to identify melanoma risk loci

To identify further loci influencing cutaneous melanoma risk and provide a more nuanced annotation of discovered cutaneous melanoma risk loci, we used a range of secondary approaches with correction for multiple testing (Online Methods). To explore the overlap

between cutaneous melanoma loci and established risk factor phenotypes, we combined our total cutaneous melanoma GWAS meta-analysis with a nevus count GWAS meta-analysis (N = 65,777; Online Methods) and separately with a UKBB hair color GWAS (N = 352,662; Online Methods). For the total cutaneous melanoma GWAS meta-analysis and nevus count the Rg is 0.57 (SE = 0.11, P-value = 2.39×10^{-7}), and for hair color scored from light hair to dark (Online Methods) the Rg is 0.290 (SE = 0.096, P-value = 0.0025). Pairwise GWAS (GWAS-PW)[38] was used to determine whether loci were associated with only one trait or pleiotropic with both cutaneous melanoma and either nevus count or hair color (Online Methods). Loci previously-reported through the combination of cutaneous melanoma and nevus GWAS[27] are now confirmed by our larger cutaneous melanoma GWAS meta-analysis (Table 2). Together these analyses identified secondary potential loci not associated at genome-wide significance levels in the total cutaneous melanoma GWAS meta-analysis. At the Bonferroni-corrected threshold of 1.25×10^{-8} (Online Methods), they included 8 loci jointly significant for cutaneous melanoma and nevus count, 17 for cutaneous melanoma and hair color, and 4 with cutaneous melanoma, nevus count and hair color (Table 3, Supplementary Table 9- 10).

In parallel, we examined data from a recently-established cell-type specific melanocyte *cis*-expression quantitative trait loci (eQTL) dataset[28] as well as tissue-based *cis*-eQTL datasets available through Genotype-Tissue Expression (GTEx)[39] resource to identify additional susceptibility loci using a transcriptome prediction mapping strategy (or transcriptome-wide association study; TWAS)[40,41]. TWAS utilizing these expression datasets enabled gene-based testing for significant *cis* genetic correlations between imputed gene expression and cutaneous melanoma risk, aiding identification of additional susceptibility loci (Online Methods). While identification of significant genes by TWAS does not establish causation, it can indicate plausible gene candidates to be utilized in pathway analyses and investigated in future functional studies. This analysis built on a previous melanocyte TWAS that analyzed data from a prior cutaneous melanoma GWAS meta-analysis[28] and identified significant novel associations between cutaneous melanoma and imputed gene expression of five genes at four loci. Importantly, the *CBWD1* locus on chromosome 9 was later identified as a genome-wide significant cutaneous melanoma+nevus count pleiotropic locus[27] (Table 3, Supplementary Table 9), and the other three loci (*ZFP90* on chromosome 16, *HEBP1* on chromosome 12, and *MSC/RP11–383H13.1* on chromosome 8) are now at genome-wide significance with cutaneous melanoma in this larger GWAS meta-analysis (Table 2). This confirmation supports the TWAS approach for both identifying new loci and nominating potentially functional genes at GWAS-discovered loci (Tables 1-2).

To empirically identify the target tissues for cutaneous melanoma risk variants, we used partitioned LD score regression[42] to determine the proportion of total cutaneous melanoma GWAS meta-analysis heritability that could be captured by genes expressed in melanocytes and in 50 GTEx tissue types. We found that partitioned cutaneous melanoma heritability was most enriched in genes specifically expressed in melanocytes (2.76-fold, $P = 3.12 \times 10^{-6}$ for top 4,000 genes; Extended Data Figure 5), followed by three other skin-related tissues (GTEx sun-exposed and non-sun-exposed skin, transformed skin fibroblasts). This enrichment was much stronger than the one based on the previously published melanoma GWAS[23]. We then focused on these four tissues for discovery of new loci, applying

Bonferroni correction for multiple comparisons based on the number of genes tested within each tissue set (Online Methods). TWAS using the melanocyte dataset (Supplementary Table 11, Supplementary Table 3) identified a total of 40 significant genes. Combining genes within 1 Mb of each other into discrete loci, 32 genes were located within 13 formally genome-wide significant cutaneous melanoma GWAS loci, and eight genes were identified within six novel loci. Considering the other skin-related tissues collectively (Supplementary Table 12, Supplementary Table 3), TWAS identified a single significant gene at one additional novel locus, as well as genes within 15 GWAS-significant loci. The TWAS using all GTEx tissues is reported in Supplementary Table 13.

In aggregate, these complementary approaches identified a total of 85 discrete loci (Figure 2; Supplementary Table 14): 54 formally significant at $P < 5 \times 10^{-8}$ in the total cutaneous melanoma meta-analysis (Table 1-2, Supplementary Table 3), and the remainder supported by one or more of the secondary analyses (Table 3-4, Supplementary Tables 7-10,14) and likely representing additional cutaneous melanoma risk loci, but requiring a larger sample size to reach genome-wide significance. In order to annotate cutaneous melanoma GWAS loci for candidate susceptibility genes for pathway analyses as well as future functional studies, we turned to eQTL colocalization analyses. These approaches identified multiple pathways that may play a role in developing melanoma and are described in the Supplementary Note.

Discussion

We report the largest cutaneous melanoma GWAS meta-analysis to date with over three times the effective sample size of prior analyses (Supplementary Table 1). We identified 68 independent cutaneous melanoma -associated variants across 54 loci. TWAS analysis, eQTL colocalization and multi-marker genomic annotations, identified promising gene candidates at many of these risk loci. Joint pairwise GWAS with the cutaneous melanoma-related traits of nevus count and hair color, and TWAS identified a further 31 independent loci that, while not formally reaching genome-wide significance for cutaneous melanoma alone, represent potential additional risk loci. Our cutaneous melanoma meta-analysis also confirmed several loci previously identified only by TWAS[28], supporting the value of TWAS in identifying additional genes associated with cutaneous melanoma (Table 4). In total, our integrative analysis identified 85 loci associated with cutaneous melanoma susceptibility (Tables 1-4, Figure 2), constituting a substantial increase from the 21 loci previously identified by cutaneous melanoma susceptibility GWAS alone (Table 1), in addition to those found by family-based approaches or in combination with nevus GWAS data (Table 2).

Our analyses showed strong genetic correlation between self-reported and clinically-confirmed cases (Supplementary Table 2; Supplementary Note), and inclusion of self-reported cases enabled the identification of 11 additional cutaneous melanoma susceptibility loci (Supplementary Tables 3,6; Supplementary Note), indicating that self-reported cutaneous melanoma cases are a valuable and reliable resource for genomic cutaneous melanoma studies. Furthermore, we assessed cutaneous melanoma genetic susceptibility across several geographic regions, including the often-underrepresented Mediterranean population. Interestingly, we found little evidence for difference in cutaneous melanoma

locus effect estimates by contributing GWAS (Supplementary Figure 2) or differences in effect size and allele frequency by geographic regions (Supplementary Figure 3), beyond minor variation in pigmentation genes (e.g., rs6059655 near *ASIP* and rs1805007 near *MC1R*). The stratified analysis based on cutaneous melanoma histological subtypes identified acral lentiginous melanomas as being uniquely unassociated with pigmentation loci, in line with observational data[29]. In contrast, the stratified analyses based on age at diagnosis and gender found no evidence for differences in the distribution of nevus-related or pigmentation-related loci.

The discovery of new loci and genes augments our understanding of cutaneous melanoma risk and provides many new insights into cutaneous melanoma etiology. Many of the loci previously associated with nevus count[27] or pigmentation[57] are also associated with cutaneous melanoma (Table 2) confirming the close relationship between these traits. Specifically, of 10 loci previously significantly-associated in a joint analysis of cutaneous melanoma and Nevus, but not associated with cutaneous melanoma alone[27], 6 are now associated with cutaneous melanoma alone (Table 2), demonstrating the benefits of conducting joint analyses. The remaining 4 loci reach $P < 5 \times 10^{-8}$ in the joint cutaneous melanoma+Nevus analysis (Supplementary Table 9); 3 of which are significant at the Bonferroni corrected threshold of 1.25×10^{-8} (Table 3). In turn, we conducted further pleiotropic analyses and identified secondary loci associated with a combination of both these traits and cutaneous melanoma, but not significantly associated with cutaneous melanoma alone (Table 3). Loci found in such joint analyses are of value as they would likely be associated with cutaneous melanoma alone in a sufficiently large cutaneous melanoma GWAS meta-analysis. These joint analyses provide a direct biological interpretation that several GWAS risk loci may act through nevus development, in line with clinical evidence. Interestingly, following these expanded pleiotropic analyses, many loci were associated with neither nevus count or hair color, indicating that many risk variants act outside of these classic cutaneous melanoma risk phenotypes (Tables 1-2).

The discovery of many new loci, when added to the existing catalog of melanoma risk loci, augments our understanding of the genetic architecture of cutaneous melanoma, as discussed in the Supplementary Note. It is important to note that confirmation of the genes we have identified are causal for cutaneous melanoma, and the biological understanding of how variants at these loci influence cutaneous melanoma, remains to be functionally established. For example, melanocyte eQTL and TWAS analyses indicated *PARP1* expression was associated with cutaneous melanoma risk SNPs at 1q42[28,58]. While *PARP1* is an established DNA repair gene, extensive functional characterization of the cutaneous melanoma risk locus over *PARP1* demonstrated that its role in cutaneous melanoma appears to be through regulation of melanocyte proliferation, senescence, and transcriptional regulation of the key melanoma oncogene *MITF*[58]. Despite the need for follow-up functional studies, a preliminary, complex model of pathways potentially important for the development of melanoma is emerging through the candidate genes suggested by this and prior work, including pathways mediating protection against UV-induced DNA damage and DNA repair, telomere maintenance, immunity, melanocyte differentiation, and cell adhesion.

For example, we identified an association between multiple independent variants at the *TP53* locus, rs78378222 and rs1641548, and cutaneous melanoma further reinforcing the potential importance of DNA repair and genome integrity for cutaneous melanoma susceptibility (see Supplementary Note). Rare germline mutations in *TP53* lead to Li-Fraumeni syndrome[59] which is associated with early onset of cancer, including cutaneous melanoma[60]. Notably, one of the common sequence variants we found to be associated with cutaneous melanoma has previously been shown to alter *TP53* mRNA levels by disruption of *TP53* polyadenylation. *TP53* responds to cellular stresses to regulate target gene expression resulting in DNA repair, cell cycle arrest, apoptosis, and cellular senescence[61,62]; variation resulting in loss of normal TP53 function could result in clonal expansion of cells that carry accumulated mutations, which may explain the association with both cutaneous melanoma and nevus count.

This study also adds to a growing body of evidence supporting a key role for telomere maintenance in cutaneous melanoma susceptibility[8,9,13,14,37,51,63], with cutaneous melanoma risk loci associated with telomere length or located near prominent telomere maintenance genes or loci, including *POT1*, *TERC*, *RTEL1*, *MPHOSPH6*, and *OBFC1*. Additional previously-identified GWAS loci are located near *CCND1* (rs4354713), *ATM* (rs1801516), and *PARP1* (rs2695237), all genes with established roles in telomere maintenance, DNA repair, and regulation of senescence[64,65].

The well-established role of immunity in melanoma biology has fueled a search for an association between variation within the HLA region and melanoma risk[66-68]. While several studies have investigated associations between HLA alleles and cutaneous melanoma, these studies have largely been conducted on small, underpowered datasets and have not been consistently replicated[69-79]. Here, we report identification of a genome-wide significant association between cutaneous melanoma susceptibility and rs28986343 at the HLA locus (see Supplementary Note). This additional evidence for a role for immunity adds to previous[28] and current TWAS and colocalization analyses suggesting association between rs408825 and expression of the innate immunity gene *MX2*. Additionally, many risk alleles for the autoimmune melanocyte-related disorder vitiligo[48,80] are protective for cutaneous melanoma with the lead SNPs either identical (rs1126809/*TYR*; rs6059655/*ASIP*), or in strong LD with cutaneous melanoma lead SNPs (rs251464 near *PPARGC1B* for vitiligo, rs32578 for melanoma, LD $r^2_{EUR} = 0.73$; rs72928038 near *BACH2* for vitiligo, rs6908626 for melanoma, $r^2_{EUR} = 0.95$; rs1129038 near *OCA2* for vitiligo, rs12913832 for melanoma, $r^2_{EUR} = 0.99$). While the vitiligo and cutaneous melanoma associations share many similar loci, suggesting a role for immunity, we cannot rule out their action on cutaneous melanoma risk being through pigmentation or protection against UV damage. Taken as a whole, these data suggest further investigation into these potentially immune-related associations, and more broadly the role of immunity in melanoma risk.

New loci emerging from these analyses suggest a role of genes or networks regulating the development and differentiation of the melanocytic lineage. The cutaneous melanoma meta-analysis identified a locus near *FOXD3*, while the pleiotropic cutaneous melanoma+Nevus analysis and TWAS locus identified a novel locus significantly associated with allelic expression of *NOTCH2* in melanocytes (Supplementary Note). *FOXD3* participates as a part

of a larger gene regulatory network governing the development of melanocytes from the neural crest, at least in part through transcriptional repression of one of the earliest markers of melanoblast development (and melanoma predisposition gene), *MITF*[81,82]. *NOTCH2*, as well as *NOTCH1*, appear to play roles in both development of the melanocyte lineage as well as maintenance of melanocyte stem cells[53,83], and NOTCH signaling has been shown to lead to de-differentiation of melanocytes to multipotent neural crest stem-like cells[84]. These two new candidate susceptibility genes join previously-identified loci also harboring genes involved in melanocyte fate. Whole-genome and targeted sequencing studies of melanoma-prone families led to the identification of a functional intermediate-penetrance missense mutation of *MITF* associated with both melanoma and nevus count (*MITF* p.E318K)[25,26], a variant that was rediscovered by this population-based meta-analysis (rs149617956, $P = 5.17 \times 10^{-25}$, OR = 0.38). Additionally, a previously-identified melanoma and nevus risk locus[85] is located ~200 kb from *SOX10,* another key regulator of melanocyte development and differentiation and direct transcriptional activator of *MITF*. These genes, and others in this gene regulatory network, have likewise been variously implicated in the progression of melanoma[86-90].

The identification of a cutaneous melanoma risk locus for which risk genotype strongly correlates with higher melanocyte-specific expression of *CDH1*, encoding E-cadherin, suggests a potential role for cell-cell adhesion in melanoma risk (see Supplementary Note). E-cadherin plays a crucial role in cell-cell adhesion, epithelial-mesenchymal transition (EMT) and carcinoma progression. Germline mutations in this gene are associated with a variety of tumors including gastric[91], breast[92], and potentially colorectal cancer[93]. In human skin, E-cadherin is typically expressed on the cell surface of both melanocytes and keratinocytes and is considered the major adhesion molecule between these two cell types[54,55]. During melanoma progression, expression of E-cadherin is typically lost, with a concurrent switch to expression of N-cadherin, facilitating preferential association with fibroblasts and vascular endothelial cells[55]. In contrast to loss of E-cadherin expression with melanoma progression, we find the cutaneous melanoma risk allele at this locus to be associated with higher expression of *CDH1*. Interestingly, melanocytes in non-lesional skin of vitiligo patients have been found to have loss of or discontinuously distributed E-cadherin expression. This loss of E-cadherin induces reduced adhesiveness to the basal layer under oxidative and mechanical stress, leading melanocytes to migrate passively to the exterior of the skin, and die by apoptosis[94]. Thus, germline variation leading to higher melanocyte *CDH1* could act as a protective mechanism, allowing cells damaged by oxidative stress to remain in the skin and survive without dying. A similar mechanism has been recently identified in breast cancer metastasis, where E-cadherin acts as a survival factor by limiting reactive oxygen-mediated apoptosis[95].

In summary, our large, international genetic meta-analysis showcases the utility of including self-reported cutaneous melanoma cases, complementary analytical approaches, and data from multiple sources to expand our understanding of cutaneous melanoma risk. While the biological mechanisms underlying many of the existing and novel cutaneous melanoma risk loci remain to be confirmed or discovered by post-GWAS functional studies and even larger GWAS, these data suggest potential pathways novel to melanoma susceptibility, and

highlight nevus formation, pigmentation and telomere maintenance, the three pathways that appear to dominate the landscape of melanoma susceptibility.

Table 1.

Loci previously identified in cutaneous melanoma susceptibility GWAS. **CHR, BP:** hg19 positional information. **rsID**: dbSNP142 rs number. **Pub**lications. We also summarize Supplementary Table 3; **Gene** prioritizes the functional target if known, followed by melanocyte or skin tissue TWAS data, or finally the closest protein coding gene; 'Multiple' indicates three or more genes. **GWS**: We indicate with yes (Y) or no (N) whether this locus is genome-wide significant ($P < 5 \times 10^{-8}$) in the total meta-analysis. The effect allele (**EA**) and non-effect allele (**NEA**) are listed, as are the effect allele **Freq**uency in the HRC reference panel[107]; total fixed-effects inverse-variance weighted meta-analysis of logistic regression two-sided P-value ($\mathbf{P_{meta}}$) and Odds Ratio (**OR**) are from an additive model and are reported per-allele with respect to the EA. Reported results are for the total meta-analysis (36,760 melanoma cases and 375,188 controls; for full details of analysis and covariates included see Online Methods). We also indicate whether this locus is associated with other traits: **Nevi**: Pleiotropically associated with cutaneous melanoma and nevus count (Online Methods; Supplementary Table 9); **Hair**: Pleiotropically associated with cutaneous melanoma and hair color (Online Methods; Supplementary Table 10). Tanning response (**Tan**) and Telomere length (**Telo**) indicates the lead SNP is associated with these traits when corrected for multiple testing (Online Methods, Supplementary Table 5).

CHR:BP	rsID	Pub	Gene	EA/ NEA	Freq	Pmeta	OR	Nevi	Hair	Tan	Telo
1:150,938,571	rs8444	[108]	Multiple	G/A	0.645	3.89×10^{-14}	1.08	-	-	Y	-
1:226,603,635	rs2695237	[27,108,109]	*PARP1*	T/C	0.628	1.53×10^{-18}	1.10	Y	-	-	-
2:38,298,139	rs1800440	[23,27]	*CYP1B1*	T/C	0.824	6.97×10^{-15}	1.10	Y	-	Y	-
2:202,143,928	rs10931936[a]	[20]	*CASP8*	T/C	0.281	2.17×10^{-8}	1.08	-	-	-	-
5:1,323,212	rs13178866[a]	[20,110,111]	*TERT*	C/T	0.554	2.59×10^{-18}	0.87	-	Y	-	Y
5:33,951,693	rs16891982[a]	[20,34,111]	*SLC45A2*	C/G	0.122	1.96×10^{-28}	0.51	-	Y	Y	-
6:21,163,919	rs6914598	[23]	*CDKAL1*	T/C	0.683	1.18×10^{-18}	0.91	-	-	Y	-
7:17,134,708	rs117132860[b]	[23,57]	*AGR3*	G/A	0.981	3.83×10^{-21}	0.71	Y	-	Y	-
9:21,803,880	rs871024[a]	[18,27]	*MTAP, CDKN2A*	C/A	0.477	2.72×10^{-23}	1.18	Y	Y	-	-
9:109,054,417	rs10739220	[23,27]	*TMEM38B*	C/T	0.260	1.34×10^{-18}	1.10	Y	Y	-	-
10:105,694,301	rs7902587	[23,27]	*OBFC1*	C/T	0.904	2.68×10^{-23}	0.86	Y	-	-	Y
11:69x,380,898	rs4354713	[20,23]	*CCND1*	A/G	0.356	8.50×10^{-21}	1.10	-	Y	-	-
11:89,017,961	rs1126809[a]	[18]	*TYR*	G/A	0.757	4.78×10^{-37}	0.83	-	Y	Y	-

CHR:BP	rsID	Pub	Gene	EA/ NEA	Freq	Pmeta	OR	Nevi	Hair	Tan	Telo
11:108,175,462	rs1801516	[20]	*ATM*	G/A	0.856	2.22×10^{-21}	1.14	Y	-	-	-
15:28,365,618	rs12913832[a]	[19,23]	*OCA2*	A/G	0.335	4.85×10^{-12}	0.88	-	Y	Y	-
16:89,986,117	rs1805007[a]	[18]	*MC1R*	C/T	0.937	5.86×10^{-52}	0.57	Y	Y	Y	-
20:32,665,748	rs6059655[a]	[17,18]	*ASIP*	A/G	0.061	2.52×10^{-42}	1.45	-	Y	Y	-
21:42,743,496	rs408825	[20]	*MX2*	C/T	0.413	1.03×10^{-32}	0.89	-	-	Y	-
22:38,545,942	rs132941	[18,27,35]	*MAFF*	T/C	0.549	8.80×10^{-23}	1.10	Y	-	Y	-

[a]Variant meta-analysis results are heterogeneous ($I^2 > 31\%$) and random effects estimates are presented.

[b]While this locus overlaps the previously reported *IRF4* or *AGR3* locus, the lead variants are independent.

Table 2.

Novel loci not previously identified in cutaneous melanoma GWAS. **CHR, BP:** hg19 position. **rsID**: dbSNP142 rs number. **Gene** prioritizes the functional target if known, followed by melanocyte or skin tissue TWAS data, or finally the closest protein coding gene; multiple indicates three or more genes (Supplementary Table 3). The effect allele (**EA**) and non-effect allele (**NEA**) are listed, as are the effect allele **Freq**uency in the HRC reference panel[107]; total fixed-effects inverse-variance weighted meta-analysis of logistic regression two-sided P-values and Odds Ratio (**OR**) are with respect to the EA. Reported results are for the total meta-analysis (36,760 melanoma cases and 375,188 controls; for full details of analysis and covariates included see Online Methods). **Nevi**: Associated with cutaneous melanoma+nevus count (Online Methods; Supplementary Table 9); **Hair**: Associated with cutaneous melanoma+hair color (Online Methods; Supplementary Table 10). Tanning response (**Tan**) and Telomere length (**Telo**) indicate lead SNP is associated with these traits when corrected for multiple testing (Online Methods, Supplementary Table 5).

CHR:BP	rsID	Gene	EA/ NEA	Freq	Pmeta	OR	Nevi	Hair	Tan	Telo
1:63,727,542	rs670318	*FOXD3*	T/C	0.047	1.21×10^{-8}	0.86	-	-	Y	-
1:154,994,978	rs76798800	*ZBTB7B, ADAM15, GBA*	G/T	0.753	3.86×10^{-15}	0.92	Y	-	Y	-
1:205,181,062	rs2369633	*DSTYK*	T/C	0.083	1.24×10^{-8}	1.10	-	-[e]	Y	-
2:25,778,637	rs12473635	*DTNB*	T/C	0.776	5.17×10^{-9}	0.93	Y	-	-	-
3:70,014,091	rs149617956[a]	*MITF*	G/A	0.998	9.00×10^{-14}	0.39	-	Y	Y	-
3:169,493,283	rs3950296[b]	*TERC*	C/G	0.747	4.47×10^{-11}	1.08	Y	-	-	Y
5:90,262,612	rs12523094[c]	*GPR98*	T/C	0.567	1.74×10^{-6c}	1.07	-	Y	Y	-
5:149,211,868	rs32578[b,d]	*PPARGC1B*	G/A	0.658	6.58×10^{-17}	1.09	Y	-	Y	-

CHR:BP	rsID	Gene	EA/ NEA	Freq	Pmeta	OR	Nevi	Hair	Tan	Telo
6:1,145,265	rs12215602[a]	*IRF4*	G/A	0.721	7.91×10^{-9}	0.94	Y	-	Y	-
6:22,719,379	rs72834823	*HDGFL1*	T/A	0.819	1.04×10^{-12}	1.10	Y	-	Y	-
6:32,748,953	rs28986343	*HLA-DQB2*	C/T	0.952	1.61×10^{-8}	1.15	-	-	-	-
6:91,005,743	rs6908626	*BACH2*	G/T	0.844	3.92×10^{-9}	1.09	-	-	-	-
7:22,115,454	rs12539524	*RAPGEF5*	C/T	0.846	1.65×10^{-8}	0.93	-	-	-	-
7:124,396,645	rs4731207	*POT1*	G/A	0.540	2.22×10^{-15}	0.93	Y	-	-	Y
7:130,738,666	rs7778378	*MKLN1*	C/T	0.248	8.93×10^{-9}	0.93	Y	Y	-	-
8:21,951,009	rs6994183	*FAM160B2*	A/T	0.866	4.84×10^{-9}	0.92	-	-	-	-
8:72,864,240	rs13263376[c]	*RP11-383H13.1, MSC*	G/A	0.364	2.28×10^{-8c}	0.93	Y	-	Y	-
9:12,587,153	rs10960710	*TYRP1*	G/T	0.393	3.08×10^{-12}	0.93	-	Y	Y	-
9:110,711,586	rs1339759[b]	*KLF4*	C/G	0.666	5.61×10^{-19}	1.10	Y	-	-	-
9:134,457,580	rs3780269	*RAPGEF1*	G/A	0.691	1.92×10^{-8}	0.94	Y	-	-	-
11:16,041,305	rs7941496	*SOX6*	G/T	0.516	1.40×10^{-9}	1.06	Y	-	Y	-
11:120,195,702	rs12290699	*TMEM136*	T/C	0.745	2.20×10^{-8}	0.94	-	-	-	-
12:13,070,752	rs1056927[b,c]	Multiple	A/G	0.561	2.74×10^{-9b}	0.93	Y	-	-	-
12:17,275,460	rs4237963	*LMO3*	T/A	0.207	1.27×10^{-9}	0.93	-	-	-	-
12:96,378,807	rs10859996	*HAL, RP11-256L6.3*	C/T	0.635	2.09×10^{-10}	1.07	-	-	-	-
12:116,580,291	rs113469387	*MED13L*	G/A	0.907	8.76×10^{-10}	0.91	-	Y	Y	-
13:113,535,949	rs1278768	*MCF2L*	G/C	0.488	6.33×10^{-12}	0.94	-	-	Y	-
15:33,277,710	rs117648907[b]	*FNM1*	C/T	0.983	7.29×10^{-12}	0.80	Y	-	-	-
16:68,822,971	rs4420522	Multiple, *CDH1*	A/G	0.690	8.34×10^{-14}	0.93	Y	Y	-	-
16:82,217,153	rs2967383	*MPHOSPH6*	G/T	0.267	2.24×10^{-9}	1.06	-	-	-	Y
17:7,571,752	rs78378222	*TP53*	T/G	0.989	3.33×10^{-10}	0.76	Y	-	-	-
19:3,540,539	rs12984831[b]	*MFSD12*	G/C	0.984	3.86×10^{-10}	0.65	Y	-	Y	-
20:62,291,767	rs143190905	*RETL1*	G/T	0.907	6.54×10^{-13}	1.15	-	-	-	Y
22:45,622,684	rs5766565	*KIAA0930*	A/G	0.647	1.44×10^{-9}	1.06	Y	Y	Y	-

CHR:BP	rsID	Gene	EA/ NEA	Freq	Pmeta	OR	Nevi	Hair	Tan	Telo
22:50,722,408	rs79966207	*PLXNB2*	T/C	0.849	8.68×10^{-9}	0.92	-	Y	-	-

[a] Associated with cutaneous melanoma by non-GWAS based approaches - *MITF*[25,26], *IRF4*[27,34,35].

[b] Previously associated pleiotropically with cutaneous melanoma and nevus count[27].

[c] Variant meta-analysis results are heterogeneous (I^2>31%) and random effects estimates are presented. For rs12523094/ *GPR98* while the lead SNP selected in conditional mapping is heterogenous, other SNPs in LD pass this requirement (e.g., rs12173258, $r^2_{EUR} = 0.9$, $P_{meta} = 1.09 \times 10^{-11}$, $I^2 = 29.6$).

[d] Previously associated with tanning response[57].

[e] Joint cutaneous melanoma+hair color P-value is greater than multiple testing corrected threshold of 1.25×10^{-8} (Supplementary Table 10).

Table 3.

Novel pleiotropic associations with cutaneous melanoma and nevus count or hair color. Reported cutaneous melanoma P-values are from the total fixed-effects inverse-variance weighted meta-analysis of logistic regression two-sided P-values from GWAS representing a total of 36,760 melanoma cases and 375,188 controls (Online Methods). Results for the lead variants from pleiotropic loci (lead SNP reaching $P < 5 \times 10^{-8}$ following a Stouffers sample size weighted meta-analysis of cutaneous melanoma P-values and either Nevus GWAS meta-analysis (N = 65,777) or Hair Color GWAS (N=352,662) and GWAS-PW Model 3 prior probability of association (PPA) > 0.5, Online Methods) distinct to those in the total cutaneous melanoma meta-analysis (Table 1, 2). **CHR, BP:** hg19 positional information. **rsID**: dbSNP142 rs number. **Gene** prioritizes genes that the variant is an eQTL for in GTEx skin datasets or otherwise is the closest protein coding gene; multiple indicates three or more genes. We report the total cutaneous melanoma meta-analysis P (**CM P**), and the **CM +nevus** or **CM+hair** color Stouffer's meta-analysis fixed effect P-value. Full results can be found in Supplementary Tables 7 and 10.

CHR:BP	rsID	Gene	CM P	CM + Nevus P	CM + Hair P
1:24787947	rs195720	*NIPAL3*	7.97×10^{-6}	-	2.24×10^{-12}
1:78450517	rs34517439	*DNAJB4*	2.23×10^{-4}	-	2.17×10^{-12}
1:214673271	rs7533482	*PTPN14*	2.79×10^{-5}	-	2.45×10^{-13}
2:135430709	rs6745983	*TMEM163*	1.69×10^{-3}	-	7.00×10^{-13}
2:214065880	rs16849932	*IKZF2*	1.46×10^{-3}	-	1.18×10^{-10}
2:240065356	rs11677464[a]	*HDAC4*	4.00×10^{-5}	1.10×10^{-9}	-
4:37470753	rs11730662	*KIAA1239*	1.82×10^{-3}	1.19×10^{-8}	-
5:56011357	rs7714232	*MAP3K1*	6.99×10^{-4}	-	3.32×10^{-22}
6:7189567	rs75818295	*RREB1*	1.87×10^{-3}	-	8.27×10^{-10}
6:11637483	rs548304	*ADTRP*	2.67×10^{-5}	-	1.46×10^{-10}
6:15503696	rs10949304	*DTNBP1*	1.7×10^{-3}	4.96×10^{-9}	-
6:50790642	rs2857482	*TFAP2B*	3.59×10^{-5}	3.44×10^{-10}	-
6:151577739, 6:151577830	rs10434895, rs10434896[b]	*AKAP12*	8.17×10^{-8}, 7.88×10^{-8}	7.71×10^{-10}	2.07×10^{-42}
8:131138979	rs111595456	*ASAP1*	3.86×10^{-4}	2.83×10^{-10}	-

CHR:BP	rsID	Gene	CM P	CM + Nevus P	CM + Hair P
9:211762, 9:235201	rs520015, rs593179[a,c]	*CBWD1*	8.95×10^{-7}, 3.78×10^{-6}	4.13×10^{-12}	1.10×10^{-43}
10:5767177	rs76154345[a]	*GDI2*	4.43×10^{-6}	7.80×10^{-11}	-
10:111889779	rs11194997	*MXI1*	3.45×10^{-6}	-	2.70×10^{-11}
11:7543519	rs11041426	*PPFIBP2*	2.73×10^{-4}	-	1.66×10^{-33}
11:62203865	rs10897275	*AHNAK*	6.47×10^{-5}	-	2.47×10^{-33}
11:91616691	rs12225068	*FAT3*	3.80×10^{-5}	-	6.48×10^{-10}
13:76351286	rs474240	*LMO7*	2.53×10^{-4}	-	9.28×10^{-9}
13:114744546	rs75414584	*RASA3*	6.31×10^{-3}	-	4.62×10^{-12}
14:64390030	rs10873172[a,d]	*SYNE2*	6.29×10^{-8}	5.95×10^{-13}	6.47×10^{-27}
14:69226931	rs11625064[d]	*ZFP36L1*	3.33×10^{-6}	2.09×10^{-10}	1.83×10^{-19}
14:92795912	rs4904871	*SLC24A4*	2.06×10^{-4}	-	2.15×10^{-278}
14:103923475	rs2273699	*MARK3*	5.27×10^{-5}	-	1.21×10^{-16}
15:48400199	rs2675345	*SLC24A5*	4.92×10^{-3}	-	1.09×10^{-9}
16:54118132, 16:54131939	rs62034121, rs62034139[d,e]	*FTO*	1.16×10^{-9}, 4.56×10^{-9}	4.69×10^{-14}	-
16:55322732	rs12930459[a]	*IRX6*	1.82×10^{-5}	4.89×10^{-9}	-

[a] Locus previously reported as pleiotropically associated with cutaneous melanoma and nevus count, but not significant for cutaneous melanoma alone here.

[b] Lead SNP for Pigment (rs10434895) and nevus (rs10434895) are in LD $r^2_{EUR} = 1.0$.

[c] Lead SNP for Pigment (rs520015) and nevus (rs593179) are in LD $r^2_{EUR} = 0.63$.

[d] Same lead SNP.

[e] Lead SNP for Pigment (rs62034121) and nevus (rs62034139) are in LD $r^2_{EUR} = 0.88$.

Table 4.

Genes identified by TWAS outside of regions identified in the total cutaneous melanoma GWAS meta-analysis. For each **gene** with a Bonferroni-corrected P-value cutoff in melanocytes ($P_{TWAS} < 3.22 \times 10^{-6}$), or skin-related tissue types ($P_{TWAS} < 5.28 \times 10^{-7}$) that does not overlap with an existing cutaneous melanoma region we report the local peak cutaneous melanoma variant from the total confirmed plus self-report GWAS meta-analysis, and TWAS **Z** score. Full results for all genes with a $P_{TWAS} < 1.48 \times 10^{-5}$ can be found in Supplementary Tables 10,12. *CBWD1* and *C9orf66* are within 1 Mb of each other and are merged into a single locus. * *RP11-676J12.7* was identified using sun-exposed skin expression data from GTEx (Supplementary Table 12), while all other genes were identified using melanocyte gene expression.

	TWAS		Locus Peak CM Variant		
Gene	Z	P	rsID	CHR:BP	CM P
NIPAL3	4.84	1.28×10^{-6}	rs2294524	1:24,770,594	2.74×10^{-7}
RCAN3	4.83	1.33×10^{-6}	rs2294524	1:24,770,594	2.74×10^{-7}
NOTCH2	4.81	1.50×10^{-6}	rs2793830	1:120,466,108	3.80×10^{-7}
PTPN14	−4.84	1.30×10^{-6}	rs6693492	1:214,685,978	2.68×10^{-5}
CBWD1	−4.81	1.51×10^{-6}	rs478882	9:205,964	1.64×10^{-6}

	TWAS		Locus Peak CM Variant		
Gene	**Z**	**P**	**rsID**	**CHR:BP**	**CM P**
C9orf66	5.05	4.48×10^{-7}	rs478882	9:205,964	1.64×10^{-6}
SYNE2	5.19	2.06×10^{-7}	rs12881652	14:64,400,120	2.12×10^{-7}
IRX6	−4.80	1.62×10^{-6}	rs12919110	16:55,319,789	1.27×10^{-6}
*RP11-676J12.7**	−5.55	2.79×10^{-8}	rs1703824	17:813,324	1.59×10^{-5}

Online Methods

Quality control metrics, imputation and association analysis

Data cleaning was performed using Illumina GenomeStudio/BeadStudio (v2.0.4 San Diego, CA, USA) and PLINK (v1.90b5.4) [96,97]. Full details of the sample collections and genotyping arrays used for each GWAS are reported in the Supplementary Note. Prior to imputation any SNP with either minor allele frequency (MAF) < 0.01, Hardy-Weinberg Equilibrium (HWE) P-value < 5 x 10^{-4} in controls or < 5 x 10^{-10} in cases was removed. Similarly, any individual was removed who was missing > 3% of variants, had heterozygosity values either > 0.05 or < −0.05 or 3 sd from the mean, whose genetically-predicted sex did not match their recorded sex, or who was determined to be non-European based on principal component analysis (PCA). In addition, one of any pair of individuals estimated to be related with identity by descent (IBD) pihat > 0.15 was removed.

The Harvard, BNMS, and 23andMe GWAS were imputed to 1000 Genomes Project phase 1 v3; for all other sets (Supplementary Table 1) imputation was conducted using the Michigan Imputation Server with the Haplotype Reference Consortium panel (HRC version 1) and run using Minimac3 [98]. Following imputation, any imputed variant with imputation quality score $r^2 < 0.5$ or MAF < 0.0001 was rejected. As rare SNPs where one allele is missing in the case or control group can lead to very large (or infinite) OR estimates, variants with an OR < 1×10^{-4} (the minimum reported by PLINK) or > 1×10^6 were also filtered. To handle variants with the same name (e.g., triplicate SNPs), variant IDs were converted to the format CHR:BP:A1A2 prior to meta-analysis.

Logistic regression under an additive model with ORs calculated on a per-allele basis was then conducted using PLINK (v1.90b5.4) [96,97] with either geographic region (in GenoMEL Phase 1 and 2 data) or principal components as covariates to account for potential population stratification. Individual studies were checked for evidence of inflation by producing QQ plots (Supplementary Figure 1) and calculating the corresponding inflation factor λ and LDSC intercept (Supplementary Table 1).

Where individual studies have deviated from this protocol, details are included in the study description in the Supplementary Note. All reported tests are two-sided.

Meta-analysis and conditional-and-joint-analysis to identify independent loci

Meta-analyses of the GWAS were conducted in one stage using both inverse-variance weighted fixed effects and random effects meta-analysis [99] as implemented in PLINK

v1.90b5.4 [96,97]. Meta-analyses were conducted for confirmed only cases, and in the total set including self-report sets (23andMe, Inc. and a portion of UK Biobank).

Conditional and joint analysis of summary GWAS meta-analysis data was performed using Genome-wide Complex Trait Analysis (GCTA, v1.26.0) to identify independently associated variants [33]. To ensure we were only detecting completely independent SNPs the collinearity threshold (--cojo-collinear) was set to $R^2 = 0.05$. The threshold for genome-wide significance 5×10^{-8} and fixed effect meta-analysis p-values and log(OR) effect sizes were analysed.

Linkage-disequilibrium (LD) between SNPs for the conditional and joint analysis of summary data in GCTA (v1.26.0) reported in the manuscript was calculated using a reference population of 5,000 individuals selected randomly from the portion of the UK Biobank population determined to be European by PCA (LD_{EUR}). Variants were converted to best guess genotype (threshold 0.3). Best guess data were cleaned for missingness > 3%, HWE $P < 1 \times 10^{-6}$, MAF < 0.001

To limit the chance of false positive claims of novel SNP/loci, we further filtered the list of 77 conditionally independent variants (Supplementary Table 4) to those (i) genome-wide significant ($P < 5 \times 10^{-8}$) in single SNP and joint conditional analysis, and (ii) as recommended[30] where there was evidence of heterogeneity between studies ($I^2 > 31\%$) the random effect P-value also needed to be $< 5 \times 10^{-8}$. Passing variants were further checked to ensure that MAFs and effect sizes were consistent across studies and that the result was not driven by a single study (Supplementary Figure 2-3). The 68 retained variants were combined into 54 loci using a concatenating 1 Mb window (Supplementary Table 3). Regional association plots for all 54 loci were interactively plotted by LDassoc (https://ldlink.nci.nih.gov/)[100] and included as Supplementary Data 1.

Multiple testing corrections

The primary aim of our study was to perform a GWAS meta-analysis of cutaneous melanoma risk. For this primary analysis our significance threshold was set at $p < 5 \times 10^{-8}$. Following this primary analysis, we conducted two classes of secondary analyses: 1) joint analysis of melanoma with a risk phenotype (Nevus or Pigmentation) and 2) TWAS.

To ensure robust adjustment for multiple testing, within the joint cutaneous melanoma-nevus and cutaneous melanoma-pigmentation GWAS analyses we Bonferroni-corrected for each of the two risk factor phenotypes (pigmentation and nevus count), as well as accounting for the two classes of secondary analysis (joint GWAS and TWAS). The resulting significance threshold was $(5 \times 10^{-8})/(2 \times 2) = 1.25 \times 10^{-8}$. Loci reaching this corrected threshold are indicated in bold in Supplementary Tables 7 and 10.

TWAS was performed on expression data from melanocytes, and then separately on the three skin tissues within GTEx (sun-exposed, not-sun-exposed, and fibroblasts) as these were the most enriched tissues in terms of enrichment for cutaneous melanoma heritability after melanocytes (Extended Data Figure 5) and are likely to be involved in cutaneous melanoma development.

For the melanocyte TWAS analysis, we Bonferroni corrected the significance threshold by the number of tested genes in melanocytes multiplied by the 2 classes of secondary tests and further for the 2 tissue sets; 0.05/(3878 genes × 2 classes × 2 tissue sets) = 3.22×10^{-6}.

For the GTEx skin TWAS analysis we Bonferroni corrected for the total number of tested genes across the tissues multiplied by two classes of secondary tests and further for the 2 tissue sets; 0.05/((8879 + 7458 + 7353 genes) × 2 classes × 2 tissue sets = 5.28×10^{-7}.

The accuracy of p-value calculation for rare SNPs where case/control numbers are imbalanced

The non-normality of the test statistics may cause severely inflated P-values due to violation of asymptotic approximations, particularly for imbalanced case-control ratios. While we addressed this for extreme cases by filtering very rare SNPs (Online Methods), we also investigated whether this could be inflating the P-value of rare SNPs included in the meta-analysis by performing 5×10^8 simulations. For each simulation, we first generated genotype data for 21 studies with the same sample size as in our meta-analysis (Supplementary Table 1) assuming Hardy Weinberg equilibrium for variants with MAF = 0.01.

We then performed association testing for each study and calculated the test statistics to derive an empirical P-value of 6.4×10^{-8} when using an asymptotic P-value of 5×10^{-8} as the threshold. While imbalanced case-control ratios had minimal impact on the calculation of asymptotic p-values for SNPs with MAF = 0.01, as the empirical P-value was slightly larger than genome-wide significance we further explored the results of our meta-analysis. Three of our 68 reported variants have a MAF less than 0.01: rs149617956 with MAF = 0.002, rs79356439 with MAF = 0.008 and rs3212371 with MAF = 0.003. All three variants had asymptotic p-values $< 5 \times 10^{-12}$. We performed 5×10^8 simulations for each of the variants using their MAF, and found no simulations had a nominal P-value $< 5 \times 10^{-12}$. These simulations indicate that the actual p-values for these three SNPs are less than $1/(5 \times 10^8) = 2 \times 10^{-9}$, and have reached genome-wide significance.

Joint analyses of cutaneous melanoma and nevus count and pigmentation

Nevus GWAS meta-analysis—Using beta meta-analysis weighted by SE as implemented in PLINK 1.90b5.4, we combined the recently published nevus meta-analysis (N = 52,506) [27] which excluded samples with melanoma but may include a small portion of overlap with the controls used for some melanoma GWAS datasets; participants of the QSkin study with nevus count that are non-overlapping and unrelated (IBD pihat < 0.15) to the QSkin melanoma case control set (N = 12,930) and the final set of participants not previously included from the Brisbane Twin Nevus Morphology study (N = 341) [27]. The total sample size was 65,777.

Pigmentation GWAS

A GWAS for hair color was performed on 352,662 UK Biobank samples not included in the melanoma GWAS who self-reported having either blonde, light brown, dark brown or black hair (coded as 1, 2, 3 and 4). Hair color was then treated as a continuous variable and

regressed on imputed genotype adjusting for principal comments using the same approach as for the melanoma GWAS.

Joint analyses—The melanoma results were then jointly analyzed first with nevus count and then with hair color. Two approaches were taken. Firstly the total confirmed plus self-report cutaneous melanoma GWAS meta-analysis results were combined with the separate nevus and pigmentation GWAS data using Stouffer's method (P-value weighted by per SNP sample N) as implemented in METAL (version 2011-03-25)[101]. LD calculations were performed in PLINK using a reference panel of 10,000 white British UK Biobank individuals as implemented in the FUMA platform (v1.3.5)[102] was used to identify independent SNPs with $P < 5 \times 10^{-8}$; independent SNPs within 1 Mb were considered to be single loci. Secondly, the melanoma and pigmentation/nevus GWAS results were analyzed using GWAS-PW (v0.21)[38], which estimates the posterior probability of four possible models for each genetic region: (i) association with cutaneous melanoma only, (ii) association with the second trait only, (iii) association with both traits (pleiotropic), (iv) association with both traits, but co-located and independent (v) no association with either trait. Given that nevus count and pigmentation are believed to act directly on melanoma risk, model (iv) seemed unrealistic so we only considered models (i), (ii), (iii) and (v). For nevus count, SNPs were assigned to blocks using the recommended boundaries for GWAS-PW (https://bitbucket.org/nygcresearch/ldetect-data). For cutaneous melanoma and hair color, 50 SNP windows were used for blocks as the default LD blocks contained multiple independent hair color loci. Following the approach taken by[27], any locus with a lead SNP reaching $P < 1.25 \times 10^{-8}$ for the combined cutaneous melanoma and nevus/hair color analysis and with a posterior probability > 0.5 that the locus is associated with both traits (model 3) to ensure that the association is not driven by a single trait was declared to be pleiotropically associated with both traits.

Analysis of pigmentation and nevi polygenic risk score across melanoma subtypes—For each subject in our study, we calculated two polygenic scores (PRS), using 276 genetic variants associated with pigmentation and 10 genetic variants associated with nevus count. Nevus count SNPs were derived from the same nevus GWAS meta-analysis used for the pleiotropic analysis (N = 65,597), with independent lead SNPs with $P < 5 \times 10^{-8}$ identified using LD calculations performed in PLINK using a reference panel of 10,000 white British UK Biobank individuals as implemented in the FUMA platform (v1.3.5)[102], with the LD r^2 cut off for independence < 0.05. Pigmentation PRS SNPs were selected from the hair color GWAS used for the pleiotropic analysis (N= 352,662), with independent lead SNPs with $P < 5 \times 10^{-8}$ and LD calculations performed in PLINK using a reference panel of 10,000 white British UK Biobank individuals as implemented in the FUMA platform, with the LD r^2 cut off for independence < 0.025. PRS were calculated for each subject by applying the regression coefficient (from the GWAS of pigmentation or nevus count) to the genotype dosages. We then tested whether PRS distribution differed between males and females, across age groups, and histology subtypes. In total, we performed 27 comparisons and thus any comparison with p-value less than 0.05/27 (=0.00186) was declared as statistically significant.

GENESIS estimation of heritability and polygenic risk

We used GENESIS (https://github.com/yandorazhang/GENESIS)[32] (Version 2019-06-01) to estimate the genetic architecture (number of causal SNPs and their effect size distribution) using the summary level statistics from the GWAS meta-analysis. Quantile-quantile plot comparing the p-values generated from this fitted distribution against the observed p-values suggested a three component Gaussian mixture model for the effect size distribution. Based on this estimated genetic architecture, we calculated the heritability at the observational scale and the number of SNPs reaching genome-wide significance for a given GWAS with known sample size. Similarly, GENESIS calculated the AUC for an additive polygenic risk prediction model built based on a discovery GWAS of known sample size.

UK Biobank melanoma risk phenotype GWAS—Four pigmentary GWAS were performed on UK Biobank participants not included in the melanoma GWAS (1) Ease of tanning with 367,229 UK Biobank samples who self-reported their ability to tan as either ‘Get very tanned’, ‘Get moderately tanned’, ‘Get mildly or occasionally tanned’ or ‘Never tan, only burn’ (coded as 1, 2, 3 and 4). Ease of tanning was treated as a continuous variable and regressed on imputed genotypes adjusting for principal components using the same approach as for the melanoma GWAS of UK Biobank data. (2) Skin color with 370,260 UK Biobank samples who self-reported having either ‘Very fair’, ‘Fair’, ‘Light olive’, ‘Dark olive’, ‘Brown’, or ‘Black’ skin color (coded as 1, 2, 3 and 4). Skin color was treated as a continuous variable and regressed on imputed genotype adjusting for principal components using the same approach as for the melanoma GWAS of UK Biobank data. (3) Number of childhood sunburns with 320,345 UK Biobank samples who self-reported their sunburn incidents pre-sixteen years old. The data were dichotomized into none and at least one pre-sixteen sunburn incident categories (coded as 1, 2). Number of childhood sunburns was treated as a binary variable and regressed using a logistic model on imputed genotype adjusting for principal comments using the same approach as for the melanoma GWAS of UK Biobank data. (4) Red hair with 120,925 UK Biobank samples who self-reported having either ‘red hair’ or other (coded as 1 or 2). Red hair was treated as a binary variable and regressed using a logistic model on imputed genotype adjusting for principal comments using the same approach as for the melanoma GWAS of UK Biobank data.

Linkage disequilibrium (LD) score regression—As LD score regression (LDSC) is sensitive to the quality of input SNPs, GWAS or meta-analysis variants were filtered to the list of high quality HapMap SNPs provided[103]. Using LD Score regression v1.0.0 genomic inflation (Lambda), intercept and SNP-heritability (h^2) were estimated. h^2 estimates were converted to the liability scale using the lifetime population prevalence for cutaneous melanoma in Australia (0.0588)[104].

LD score regression of tissue-specific genes—Cutaneous melanoma heritability enrichment for SNPs around tissue-specific genes was assessed by stratified LD score regression as described previously [28,42] and implemented in the LDSC program v1.0.0 (https://github.com/bulik/ldsc). Briefly, RNA-seq data for all 50 GTEx (v7) tissue types and primary melanocyte were quantified as RPKM using RNA-SeQC (v1.18) [105] and quantile normalized to reduce batch effect. Tissue-specific genes were defined by calculating the t-

statistic of each gene for a given tissue, excluding all samples from the same tissue category. Tissue category assignment for GTEx tissue types was based on the previous publications [28,106], and melanocytes were defined as "skin" category together with two types of skin and transformed skin fibroblasts from the GTEx. We selected the top 1,000, 2,000, and 4,000 tissue-specific genes from the t-statistic analysis, and added 100 Kb each to the transcription start site and transcription end site to define tissue-specific genes annotation. Stratified LD score regression was then applied on a joint SNP annotation to estimate the heritability enrichment against the total cutaneous melanoma GWAS data from the current study.

Colocalization of cutaneous melanoma GWAS and eQTLs—We performed colocalization analyses of cutaneous melanoma GWAS signals with eQTL signals from our melanocyte and 48 GTEx (v7) tissue eQTL datasets (note that 2 tissue types that were included for LDSC using expression data were not included here as well as in TWAS analyses due to lack of eQTL data from GTEx), using eQTL and GWAS CAusal Variants Identification in Associated Regions (eCAVIAR, v2.0, http://genetics.cs.ucla.edu/caviar/, https://github.com/fhormoz/caviar)[43]. Consistent with the previous study, we used 50 SNPs upstream and downstream of each cutaneous melanoma GWAS lead SNP to extract both GWAS and eQTL summary statistics to be used as the input for eCAVIAR analysis. The LD matrix was calculated using the unphased 1000 Genomes reference set. For the CLPP score calculation, we allowed a maximum number of two causal SNPs in each locus. For a given cutaneous melanoma GWAS locus, an eGene with a CLPP score above 1% (0.01) was considered to display a positive co-localization. To avoid reporting spurious effects, we applied a conservative criterion and only reported variants displaying LD $r^2 > 0.9$ with the cutaneous melanoma GWAS lead SNP and eQTL P-value below a Bonferroni-corrected cutoff of each dataset (0.05/number of eGenes tested for each tissue dataset).

TWAS—We performed transcriptome-wide association studies (TWAS) for the cutaneous melanoma GWAS meta-analysis data using TWAS/FUSION (http://gusevlab.org/projects/fusion/) as previously described[28,41]. TWAS was performed in three separate groups, using eQTL datasets from 1) melanocytes, 2) three skin tissues (sun-exposed, not-sun-exposed, and fibroblasts) within GTEx (V7), and 3) the rest of GTEx tissue types (a total of 45) by imputing the gene expression phenotypes for the total cutaneous melanoma GWAS meta-analysis data. The analysis parameters were set to allow for multiple prediction models, independent reference LD, additional feature statistics and cross-validation results[41]. The total cutaneous melanoma GWAS meta-analysis summary statistics were included with no significance thresholding. For GTEx data, we downloaded the precomputed expression reference weights for GTEx gene expression (v7) RNA-seq across 48 tissue types from the TWAS/FUSION website (http://gusevlab.org/projects/fusion/). We computed functional weights from the primary melanocyte RNA-seq data[28] one gene at a time. Genes that failed quality control during the heritability check (using minimum heritability P-value 0.01) were excluded from further analyses. We restricted the *cis*-locus to 500 Kb on either side of the gene boundary.

Data Availability—Genome-wide summary statistics for the confirmed meta-analysis have been made publicly available at dbGaP (phs001868.v1.p1), with the exclusion of genomic

data from 23andMe. Results for SNPs with a fixed or random $P < 5 \times 10^{-7}$, from the total meta-analysis are reported in Supplementary Table 7. The total meta-analysis includes self-report cutaneous melanoma GWAS data from the UK Biobank and 23andMe. The raw genetic and phenotypic UK Biobank data used in this study, which were used under license, are available from: http://www.ukbiobank.ac.uk/. The genome-wide summary statistics from 23andMe, Inc. data were obtained under a data transfer agreement. Further information about obtaining access to the 23and Me, Inc. summary statistics are available from: https://research.23andme.com/collaborate/.

Extended Data

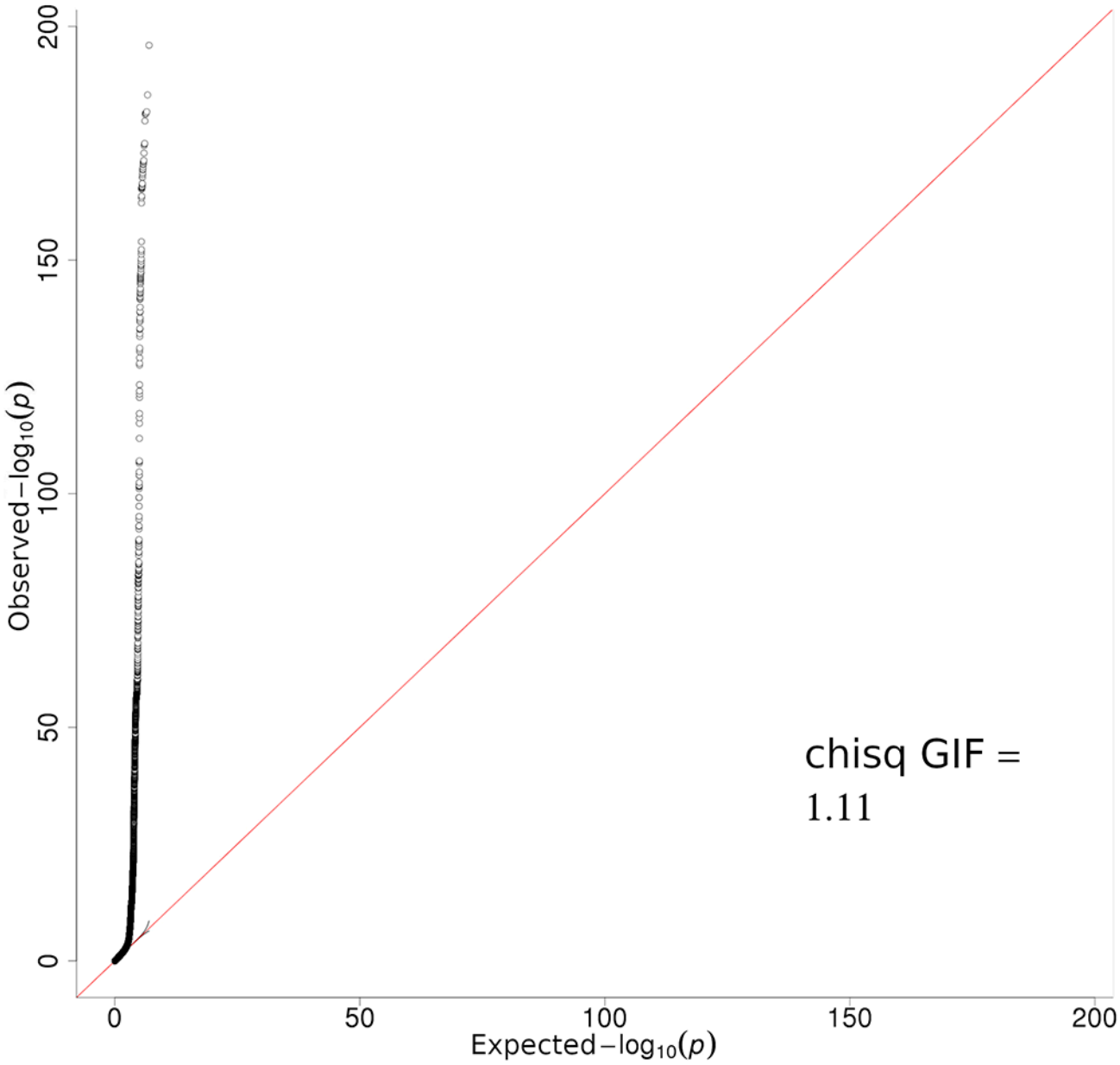

Extended Data Fig. 1. Quantile-Quantile plot of total CM meta-analysis.

Quantile-quantile plots of negative $\log_{10}$ two sided P-value derived from a fixed-effects inverse-variance weighted meta-analysis of log(OR) effect-sizes derived from the logistic regression GWAS listed in Supplementary Table 1. All confirmed and self-report cases are included, with a total sample size of 36,760 melanoma cases and 375,188 controls.

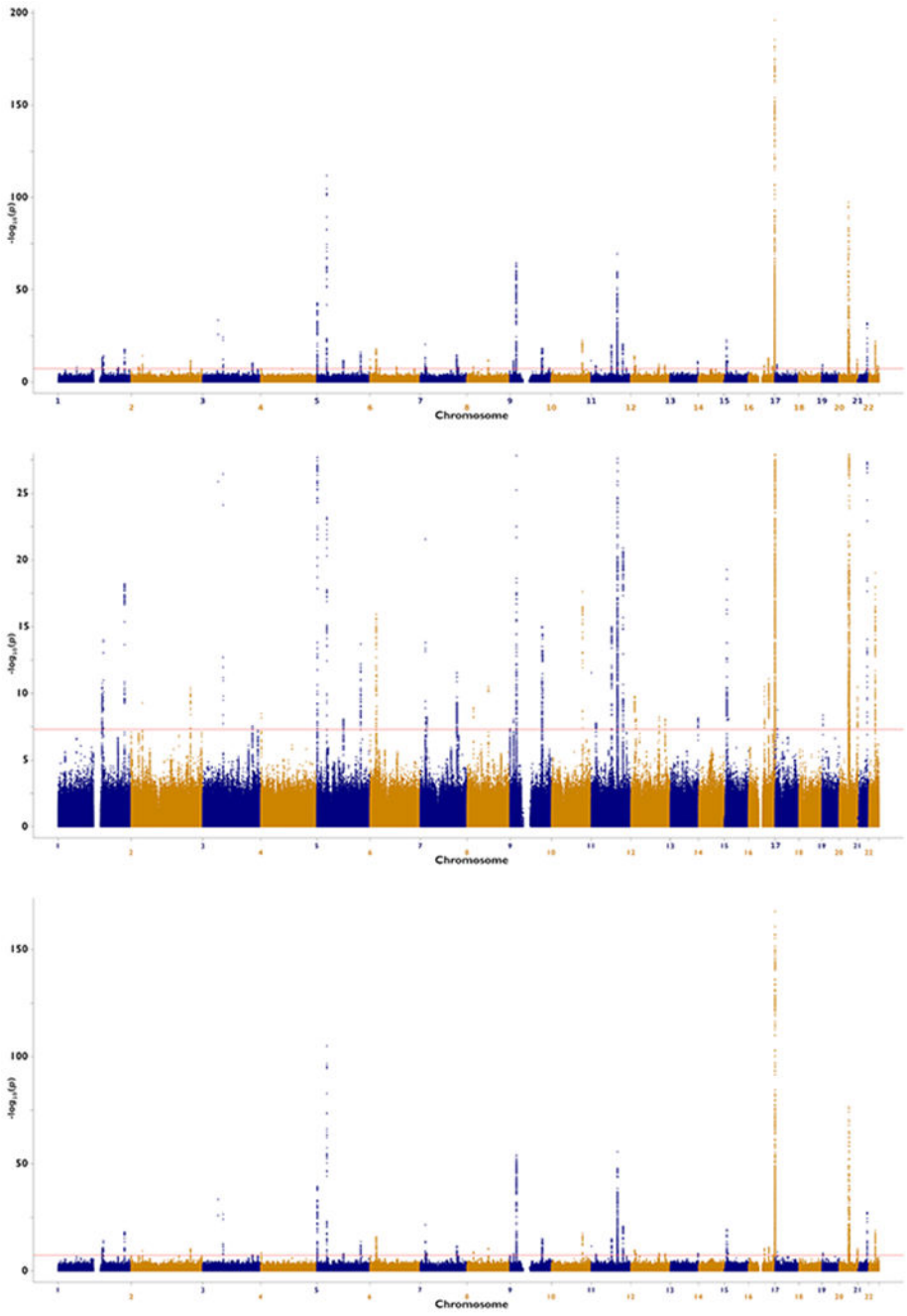

Extended Data Fig. 2. Manhattan plots of melanoma risk loci from total and confirmed-only GWAS-meta-analyses.

Negative $\log_{10}$ two sided P-value derived from a fixed-effects inverse-variance weighted meta-analysis of log(OR) effect-sizes derived from the logistic regression GWAS (y-axis) are plotted by their chromosome position. The confirmed-only analysis included 30,134 cases with histopathologically confirmed CM, and 81,415 controls. The total CM meta-analysis includes all confirmed and self-report cases, with a total sample size of 36,760 CM cases and 375,188 controls. Multiple-testing corrected genome-wide significance threshold was $P<5\times10^{-8}$. We display in order the total CM meta-analysis without limiting the y-axis;

the pathologically confirmed CM cases only meta-analysis with the y-axis limited to 1×10^{-25} and without a limit to more clearly display loci other than *MC1R.*

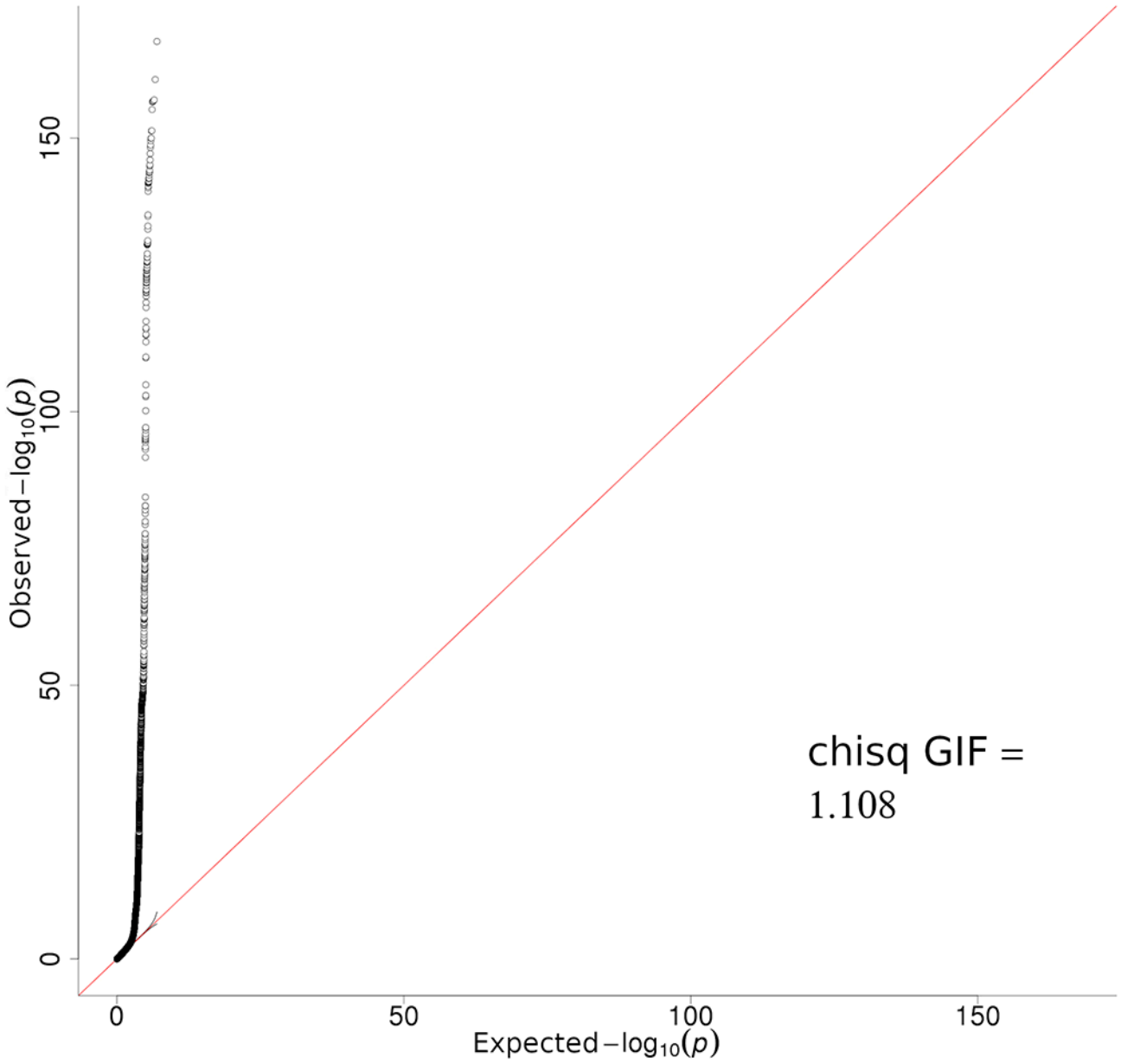

Extended Data Fig. 3. Quantile-Quantile plot of confirmed-only CM meta-analysis.
Quantile-quantile plots of negative $\log_{10}$ two sided P-value derived from a fixed-effects inverse-variance weighted meta-analysis of log(OR) effect-sizes derived from the logistic regression GWAS listed in Supplementary Table 1. Only cases with histopathologically confirmed CM are included, with a total sample size of 30,134 melanoma cases and 81,415 controls.

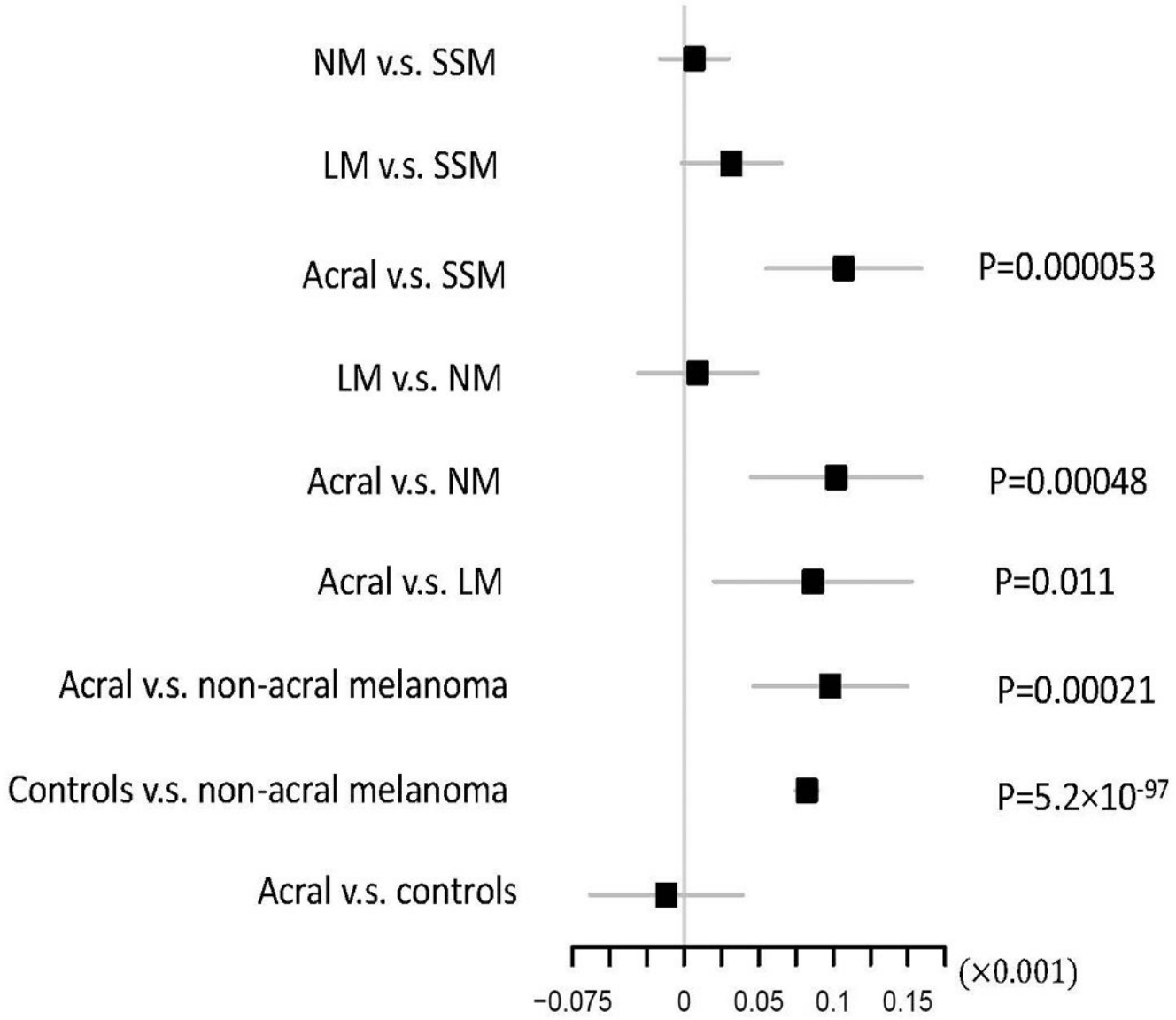

Extended Data Fig. 4. Distribution of pigmentation polygenic risk scores across melanoma histological subtypes.

The figure shows whether PRS defined based on SNPs associated with hair colour differ across CM histological types (Online Methods; SSM: superficial spreading melanoma; NM: nodular melanoma; LM: lentigo melanoma; Acral: acral lentiginous melanoma). The higher the PRS the lighter the hair colour. When comparing subtype 1 vs. subtype 2, we report the effect size for the linear regression of PRS on subtype 1, including study and principal components as covariates to control for population stratification. The regression coefficient, 95% confidence interval, and statistical significance are shown. The positive beta indicates the PRS is higher in subtype 2 (e.g., non-acral melanomas). This analysis included 9828 SSM, 2137 NM, 900 LM, 353 acral melanoma cases and 44676 controls. Two-sided t-statistic was used for testing significance. P-values reported were not adjusted for multiple comparison.

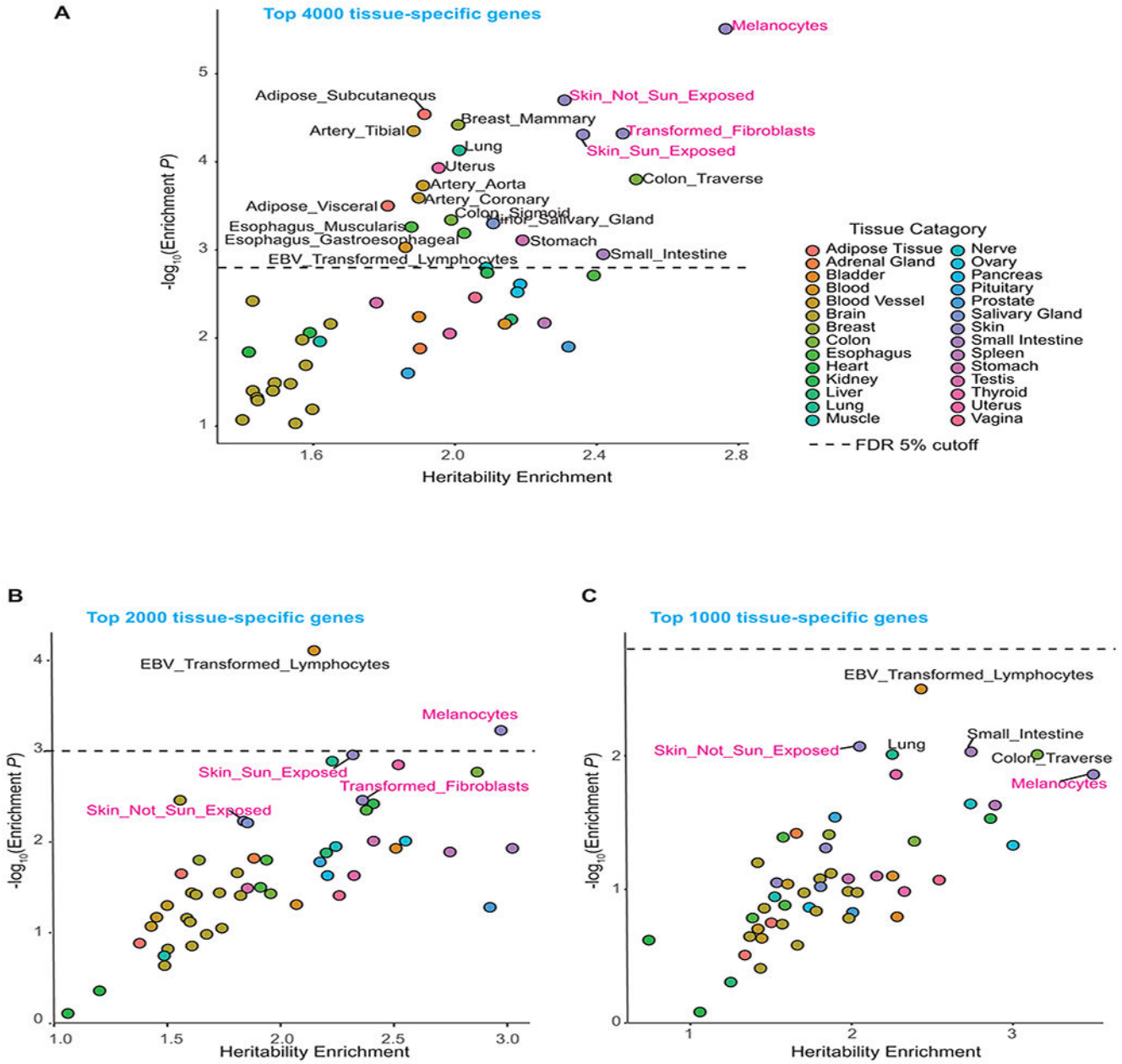

Extended Data Fig. 5. LD score regression plots.

LD score regression was performed for the top 4000 (A) 2000 (B) and 1000 (C) tissue-specific genes from melanocyte and GTEx tissue types (v7 datasets), to assess the enrichment of melanoma heritability in these genomic regions using summary statistics from Total CM GWAS meta-analysis. The level of enrichment and P-values are shown, with an FDR = 0.05 cutoff marked as a dashed horizontal line (See Online Methods for statistical test). Tissue categories are color-coded, and a subset of top individual tissue types are shown on the plot. Tissue types from “Skin” category including melanocytes are highlighted in magenta.

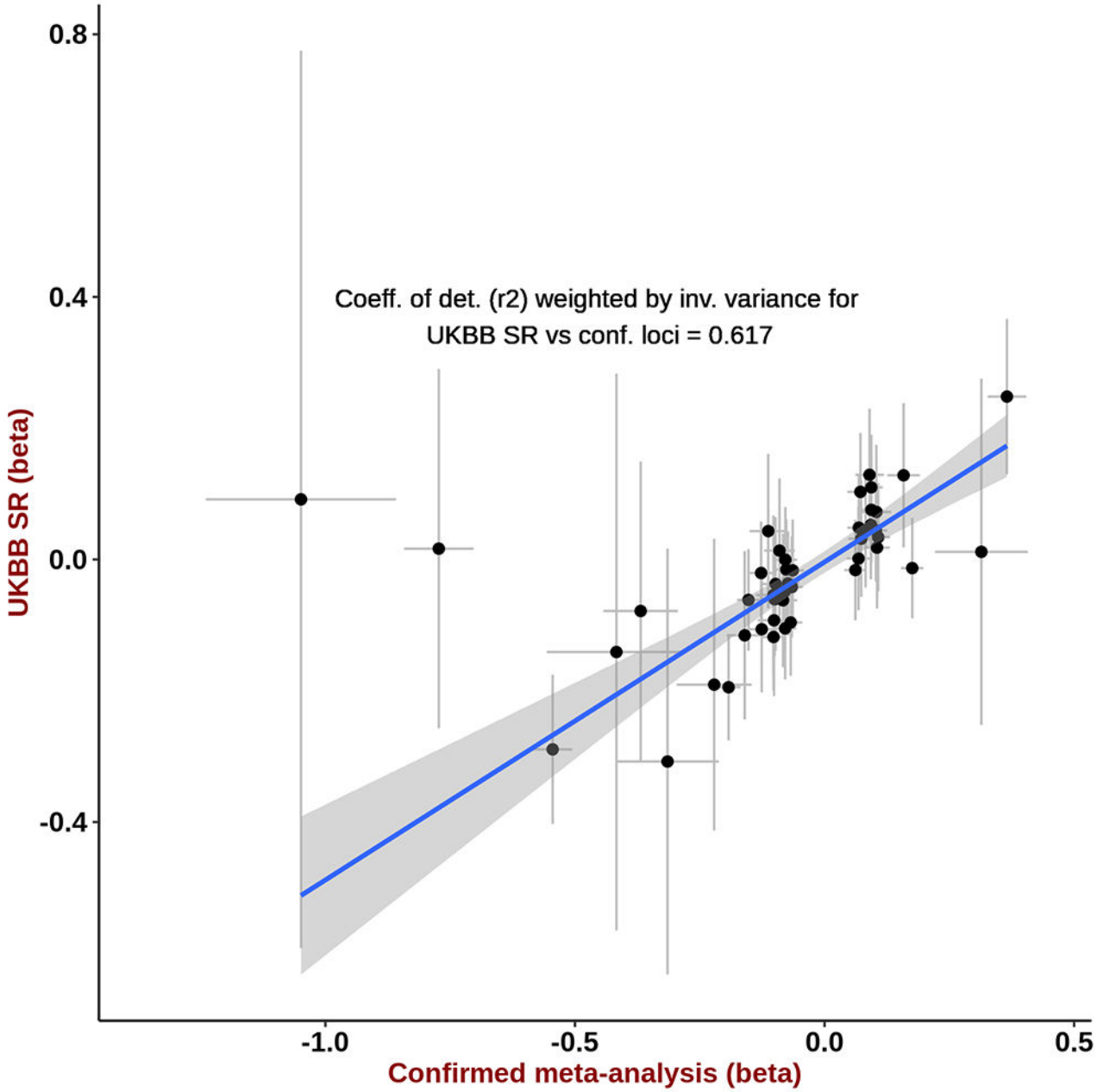

Extended Data Fig. 6. Effect sizes for confirmed-only meta-analysis versus UKBB self-report set

For each independent genome-wide significant ($P<5\times10^{-8}$) lead SNP from the confirmed only meta-analysis (30,134 melanoma cases and 81,415 controls), we plot on the Y-axis UK Biobank self-report GWAS (UKBB SR) log(OR) and standard error from a logistic regression GWAS (1,802 self-report CM cases and 7,208 controls) and on the X-axis we plot the log(OR) and standard error from a fixed-effects inverse-variance weighted meta-analysis of log(OR) effect-sizes derived from the logistic regression GWAS for confirmed melanoma cases listed in Supplementary Table 1. We also report the r^2 correlation from the linear regression of UKBB SR log(OR) on the confirmed met-analysis estimates, weighted by their standard error.

Supplementary Material

Refer to Web version on PubMed Central for supplementary material.

Authors

Maria Teresa Landi[1,*,@], D. Timothy Bishop[2,*], Stuart MacGregor[3,*], Mitchell J. Machiela[1,*], Alexander J. Stratigos[4,#], Paola Ghiorzo[5,#], Myriam Brossard[6], Donato Calista[7], Jiyeon Choi[1], Maria Concetta Fargnoli[8], Tongwu Zhang[1], Monica Rodolfo[9], Adam J. Trower[10], Chiara Menin[11], Jacobo Martinez[12], Andreas Hadjisavvas[13], Lei Song[1], Irene Stefanaki[14], Richard Scolyer[15,16,17,18], Rose Yang[1], Alisa M. Goldstein[1], Miriam Potrony[19], Katerina P. Kypreou[14], Lorenza Pastorino[20], Paola Queirolo[21], Cristina Pellegrini[8], Laura Cattaneo[22], Matthew Zawistowski[23], Pol Gimenez-Xavier[19], Arantxa Rodriguez[24], Lisa Elefanti[11], Siranoush Manoukian[25], Licia Rivoltini[9], Blair H. Smith[26], Maria A. Loizidou[13], Laura Del Regno[27,28], Daniela Massi[29], Mario Mandala[30], Kiarash Khosrotehrani[31,32], Lars A. Akslen[33,34], Christopher I. Amos[35], Per A. Andresen[36], Marie-Françoise Avril[37], Esther Azizi[38,39], H. Peter Soyer[40,32], Veronique Bataille[41], Bruna Dalmasso[5,42], Lisa M. Bowdler[43], Kathryn P. Burdon[44], Wei V. Chen[45], Veryan Codd[46,47], Jamie E. Craig[48], Tadeusz Dębniak[49], Mario Falchi[41], Shenying Fang[50], Eitan Friedman[39], Sarah Simi[29], Pilar Galan[51], Zaida Garcia-Casado[24], Elizabeth M. Gillanders[52], Scott Gordon[53], Adele Green[54,55], Nelleke A. Gruis[56], Johan Hansson[57], Mark Harland[58], Jessica Harris[59], Per Helsing[60], Anjali Henders[61], Marko Hočevar[62], Veronica Höiom[57], David Hunter[63,64], Christian Ingvar[65], Rajiv Kumar[66], Julie Lang[67], G. Mark Lathrop[68], Jeffrey E. Lee[50], Xin Li[69], Jan Lubiński[70], Rona M. Mackie[71,67], Maryrose Malt[54], Josep Malvehy[72], Kerrie McAloney[53], Hamida Mohamdi[6], Anders Molven[34,73], Eric K. Moses[74], Rachel E. Neale[75], Srdjan Novaković[76], Dale R. Nyholt[77,53], Håkan Olsson[78,79], Nicholas Orr[80], Lars G. Fritsche[81], Joan Anton Puig-Butille[82], Abrar A. Qureshi[83], Graham L. Radford-Smith[84,85,86], Juliette Randerson-Moor[58], Celia Requena[24], Casey Rowe[31], Nilesh J. Samani[46,47], Marianna Sanna[41], Dirk Schadendorf[87,88], Hans-Joachim Schulze[89], Lisa A. Simms[84], Mark Smithers[90,91], Fengju Song[92], Anthony J. Swerdlow[93,94], Nienke van der Stoep[95], Nicole A. Kukutsch[56], Alessia Visconti[41], Leanne Wallace[61], Sarah V. Ward[96,97], Lawrie Wheeler[59], Richard A. Sturm[40], Amy Hutchinson[1,98], Kristine Jones[1,98], Michael Malasky[1,98], Aurelie Vogt[1,98], Weiyin Zhou[1,98], Karen A. Pooley[99], David E. Elder[100], Jiali Han[69], Belynda Hicks[1,98], Nicholas K. Hayward[101], Peter A. Kanetsky[102], Chad Brummett[103], Grant W. Montgomery[104], Catherine M Olsen[105], Caroline Hayward[106], Alison M. Dunning[107], Nicholas G. Martin[53], Evangelos Evangelou[108,109], Graham J. Mann[110], Georgina Long[15,111], Paul D. P. Pharoah[107], Douglas F. Easton[99], Jennifer H. Barrett[10], Anne E. Cust[110,112], Goncalo Abecasis[113], David L. Duffy[53,114], David C. Whiteman[105], Helen Gogas[115], Arcangela De Nicolo[116], Margaret A. Tucker[1], Julia A. Newton Bishop[58], GenoMEL Consortium[117], Q-MEGA and QTWIN Investigators[117], ATHENS Melanoma Study Group[117], 23andMe[117], The SDH Study Group[117], IBD Investigators[117], Essen-Heidelberg Investigators[117], AMFS Investigators[117], MelaNostrum Consortium[117], Ketty Peris[27,28], Stephen J.

Chanock[1], Florence Demenais[6], Kevin M. Brown[1,#], Susana Puig[19,#], Eduardo Nagore[24,#], Jianxin Shi[1,*], Mark M. Iles[10,*,@], Matthew H. Law[3,*,@]

Affiliations

[1]Division of Cancer Epidemiology and Genetics, National Cancer Institute, National Institutes of Health, Bethesda, Maryland, USA [2]Leeds Institute of Medical Research at St James's, University of Leeds, Leeds, UK & Leeds Institute for Data Analytics, University of Leeds, Leeds, UK [3]Statistical Genetics, QIMR Berghofer Medical Research Institute, Brisbane, Australia [4]Department of Dermatology, Andreas Syggros Hospital, Medical School, National and Kapodistrian University of Athens, Athens, Greece [5]Genetics of Rare Cancers, Department of Internal Medicine (DiMI), University of Genoa and Ospedale Policlinico San Martino Genoa, Genoa, Italy [6]Institut National de la Santé et de la Recherche Médicale (INSERM), UMRS-1124, Genetic Epidemiology and Functional Genomics of Multifactorial Diseases Team, Université Paris Descartes, Paris, France [7]Department of Dermatology, Maurizio Bufalini Hospital, Cesena, Italy [8]Department of Dermatology, Department of Biotechnological and Applied Clinical Sciences, University of L'Aquila, L'Aquila, Italy [9]Unit of Immunotherapy of Human Tumors, Department of Research, Fondazione IRCCS Istituto Nazionale dei Tumori di Milano, Italy [10]Leeds Institute for Data Analytics, University of Leeds, Leeds, UK [11]Immunology and Molecular Oncology Unit, Veneto Institute of Oncology IOV - IRCCS, Padua, Italy [12]Red Valenciana de Biobancos, FISABIO [13]Department of EM/Molecular Pathology & The Cyprus School of Molecular Medicine, The Cyprus Institute of Neurology and Genetics, Nicosia, Cyprus [14]Department of Dermatology, University of Athens School of Medicine, Andreas Sygros Hospital, Athens, Greece [15]Melanoma Institute Australia, The University of Sydney, Sydney, Australia [16]Royal Prince Alfred Hospital, Sydney, NSW, Australia [17]The University of Sydney, Central Clinical School, Sydney, NSW, Australia [18]New South Wales Health Pathology, Sydney, NSW, Australia [19]Dermatology Department, Melanoma Unit, Hospital Clínic de Barcelona, IDIBAPS, Universitat de Barcelona, Centro de Investigación Biomédica en Red de Enfermedades Raras (CIBERER), Barcelona, Spain [20]Genetics of Rare Cancers, Department of Internal Medicine (DiMI), University of Genoa and Policlinico San Martino Research Hospital Genoa, Genoa, Italy [21]Medical Oncology, Ospedale Policlinico San Martino Genoa, Genoa, Italy [22]Pathology Unit, Azienda Socio-Sanitaria Territoriale Papa Giovanni XXIII, Bergamo, Italy [23]Department of Biostatistics, University of Michigan School of Public Health, Ann Arbor, MI 48109, USA; Center for Statistical Genetics, University of Michigan School of Public Health, Ann Arbor, MI 48109, US [24]Department of Dermatology, Instituto Valenciano de Oncología, València, Spain [25]Unit of Medical Genetics, Department of Medical Oncology and Hematology, Fondazione IRCCS Istituto Nazionale dei Tumori di Milano, Italy [26]Division of Population Health and Genomics, Ninewells Hospital and Medical School, University of Dundee, Dundee DD1 9SY, United Kingdom [27]Institute of Dermatology, Catholic University, Rome, Italy [28]Fondazione Policlinico Universitario A. Gemelli, IRCCS-Rome, Italy [29]Section of Anatomic Pathology, Department of Health Sciences, University of Florence, Italy [30]Department of

Oncology, Giovanni XXIII Hospital, Bergamo, Italy [31]The University of Queensland, UQ Diamantina Institute, Brisbane Australia [32]Department of Dermatology, Princess Alexandra Hospital, Brisbane, Australia [33]Centre for Cancer Biomarkers CCBIO, Department of Clinical Medicine, University of Bergen, Bergen, Norway [34]Department of Pathology, Haukeland University Hospital, Bergen, Norway [35]Department of Community and Family Medicine, Geisel School of Medicine, Dartmouth College, Hanover, New Hampshire, USA [36]Department of Pathology, Molecular Pathology, Oslo University Hospital, Rikshospitalet, Oslo, Norway [37]Assistance Publique–Hôpitaux de Paris, Hôpital Cochin, Service de Dermatologie, Université Paris Descartes, Paris, France [38]Department of Dermatology, Sheba Medical Center, Tel Hashomer, Sackler Faculty of Medicine, Tel Aviv, Israel [39]Oncogenetics Unit, Sheba Medical Center, Tel Hashomer, Sackler Faculty of Medicine, Tel Aviv University, Tel Aviv, Israel [40]Dermatology Research Centre, The University of Queensland Diamantina Institute, Translational Research Institute, Brisbane, Qld 4102, Australia [41]Department of Twin Research and Genetic Epidemiology, King's College London, London, SE1 7EH, UK Plus, for Veronique: Department of Dermatology, West Herts NHS Trust, Herts, HP2 4AD, UK [42]Laboratory of Genetics of Rare Cancers, Istituto di ricovero e cura a carattere scientifico Azienda Ospedaliera Universitaria (IRCCS AOU) San Martino-IST Istituto Nazionale per la Ricerca sul Cancro, Genoa, Italy [43]Sample Processing, QIMR Berghofer Medical Research Institute, Brisbane, Australia [44]Menzies Institute for Medical Research, University of Tasmania, Hobart, Tasmania, Australia [45]Department of Genetics, The University of Texas MD Anderson Cancer Center, Houston, Texas, USA [46]Department of Cardiovascular Sciences, University of Leicester, Leicester, UK [47]NIHR Leicester Biomedical Research Centre, Glenfield Hospital, Leicester, UK [48]Department of Ophthalmology, Flinders University, Adelaide, Australia [49]Department of Genetics and Pathology, International Hereditary Cancer Center, Pomeranian Medical University, Szczecin, Poland [50]Department of Surgical Oncology, The University of Texas MD Anderson Cancer Center, Houston, Texas, USA [51]Université Paris 13, Equipe de Recherche en Epidémiologie Nutritionnelle (EREN), Centre de Recherche en Epidémiologie et Statistiques, Institut National de la Santé et de la Recherche Médicale (INSERM U1153), Institut National de la Recherche Agronomique (INRA U1125), Conservatoire National des Arts et Métiers, Communauté d'Université Sorbonne Paris Cité, F-93017 Bobigny, France [52]Inherited Disease Research Branch, National Human Genome Research Institute, National Institutes of Health, Baltimore, Maryland, USA [53]Genetic Epidemiology, QIMR Berghofer Medical Research Institute, Brisbane, Australia [54]Cancer and Population Studies, QIMR Berghofer Medical Research Institute, Brisbane, Australia [55]CRUK Manchester Institute and Institute of Inflammation and Repair, University of Manchester, Manchester, UK [56]Department of Dermatology, Leiden University Medical Centre, Leiden, The Netherlands [57]Department of Oncology-Pathology, Karolinska Institutet, Karolinska University Hospital, Stockholm, Sweden [58]Leeds Institute of Medical Research at St James's, University of Leeds, Leeds, UK [59]Translational Research Institute, Institute

of Health and Biomedical Innovation, Princess Alexandra Hospital, Queensland University of Technology, Brisbane, Australia [60]Department of Dermatology, Oslo University Hospital, Rikshospitalet, Oslo, Norway [61]Institute for Molecular Bioscience, The University of Queensland, Brisbane, Australia. [62]Department of Surgical Oncology, Institute of Oncology Ljubljana, Ljubljana, Slovenia [63]University of Oxford, Nuffield Department of Population Health, Oxford, UK [64]Harvard T.H. Chan School of Public Health, Program in Genetic Epidemiology and Statistical Genetics, Boston, MA, USA [65]Department of Surgery, Clinical Sciences, Lund University, Lund, Sweden [66]Division of Molecular Genetic Epidemiology, German Cancer Research Center, Im Neuenheimer Feld 580, Heidelberg Germany [67]Department of Medical Genetics, University of Glasgow, Glasgow, UK [68]McGill University and Genome Quebec Innovation Centre, Montreal, Canada [69]Department of Epidemiology, Richard M. Fairbanks School of Public Health, Melvin and Bren Simon Cancer Center, Indiana University, Indianapolis, USA [70]International Hereditary Cancer Center, Pomeranian Medical University, Szczecin, Poland [71]Department of Public Health, University of Glasgow, Glasgow UK [72]Dermatology Department, Melanoma Unit, Hospital Clínic de Barcelona, IDIBAPS, Universitat de Barcelona, Centro de Investigación Biomédica en Red en Enfermedades Raras (CIBERER), Barcelona, Spain [73]Gade Laboratory for Pathology, Department of Clinical Medicine, University of Bergen, Bergen, Norway [74]Centre for Genetic Origins of Health and Disease, Faculty of Medicine, Dentistry and Health Sciences, The University of Western Australia, Western Australia, Australia [75]Cancer Aetiology & Prevention, QIMR Berghofer Medical Research Institute, Brisbane, Australia [76]Department of Molecular Diagnostics, Institute of Oncology Ljubljana, Ljubljana, Slovenia [77]School of Biomedical Sciences and Institute of Health and Biomedical Innovation, Queensland University of Technology, Brisbane, Queensland, Australia [78]Department of Oncology/Pathology, Clinical Sciences, Lund University, Lund; Sweden [79]Department of Cancer Epidemiology, Clinical Sciences, Lund University, Lund, Sweden [80]Breakthrough Breast Cancer Research Centre, The Institute of Cancer Research, London, UK [81]Center for Statistical Genetics, Department of Biostatistics, University of Michigan School of Public Health, Ann Arbor, MI, USA [82]Biochemistry and Molecular Genetics Department, Melanoma Unit, Hospital Clínic de Barcelona, IDIBAPS, Universitat de Barcelona, Centro de Investigación Biomédica en Red en Enfermedades Raras (CIBERER), Barcelona, Spain [83]Department of Dermatology, The Warren Alpert Medical School of Brown University, Rhode Island, USA [84]Inflammatory Bowel Diseases, QIMR Berghofer Medical Research Institute, Brisbane, Australia [85]Department of Gastroenterology and Hepatology, Royal Brisbane & Women's Hospital, Brisbane, Australia [86]University of Queensland School of Medicine, Herston Campus, Brisbane, Australia [87]Department of Dermatology, University Hospital Essen, Essen, Germany [88]German Consortium Translational Cancer Research (DKTK), Heidelberg, Germany [89]Department of Dermatology, Fachklinik Hornheide, Institute for Tumors of the Skin at the University of Münster, Münster, Germany [90]Queensland Melanoma Project, Princess Alexandra Hospital, The University of Queensland,

Australia [91]Mater Research Institute, The University of Queensland, Australia. [92]Departments of Epidemiology and Biostatistics, Key Laboratory of Cancer Prevention and Therapy, Tianjin, National Clinical Research Center of Cancer, Tianjin Medical University Cancer Institute and Hospital, Tianjin, P. R. China [93]Division of Genetics and Epidemiology, The Institute of Cancer Research, London, UK [94]Division of Breast Cancer Research, The Institute of Cancer Research, London, UK [95]Department of Clinical Genetics, Center of Human and Clinical Genetics, Leiden University Medical Center, Leiden, The Netherlands [96]Centre for Genetic Origins of Health and Disease, School of Biomedical Sciences, The University of Western Australia, Perth, Australia [97]Department of Epidemiology and Biostatistics, Memorial Sloan Kettering Cancer Center, New York, New York, USA [98]Cancer Genome Research Laboratory, Leidos Biomedical Research Inc., Bethesda, Maryland, USA [99]Centre for Cancer Genetic Epidemiology, Department of Public Health and Primary Care, University of Cambridge, Cambridge, UK [100]Department of Pathology and Laboratory Medicine, Perelman School of Medicine at the University of Pennsylvania, Philadelphia, Pennsylvania, USA [101]Oncogenomics, QIMR Berghofer Medical Research Institute, Brisbane, Australia [102]Department of Cancer Epidemiology, H. Lee Moffitt Cancer Center and Research Institute, Tampa, Florida, USA [103]Department of Anesthesiology, University of Michigan, Ann Arbor, MI, USA [104]Molecular Biology, the University of Queensland, Brisbane, Australia. [105]Cancer Control Group, QIMR Berghofer Medical Research Institute, Brisbane, Australia [106]MRC Human Genetics Unit, Institute of Genetics and Molecular Medicine, University of Edinburgh, Western General Hospital, Edinburgh EH42 XU, United Kingdom [107]Centre for Cancer Genetic Epidemiology, Department of Oncology, University of Cambridge, Cambridge, UK [108]Department of Hygiene and Epidemiology, University of Ioannina Medical School, Ioannina, Greece [109]Department of Epidemiology and Biostatistics, Imperial College London, London, UK [110]Centre for Cancer Research, Westmead Institute for Medical Research, and The Melanoma Institute, The University of Sydney, Sydney, Australia [111]Royal North Shore Hospital, Sydney Australia [112]Cancer Epidemiology and Prevention Research, Sydney School of Public Health, and The Melanoma Institute, University of Sydney, Sydney, Australia [113]Department of Biostatistics, University of Michigan, Ann Arbor, 48109, MI, USA [114]The University of Queensland Diamantina Institute, The University of Queensland, Woolloongabba, QLD 4102, Australia [115]First Department of Internal Medicine, Laikon General Hospital Greece, National and Kapodistrian University of Athens, Athens, Greece [116]Cancer Genomics Program, Veneto Institute of Oncology IOV - IRCCS, Padua, Italy [117]A full list of members and affiliations appears in the Supplementary Note

Acknowledgments

NCI

This study was supported by the Intramural Research Program of the Division of Cancer Epidemiology and Genetics, National Cancer Institute, National Institutes of Health, Department of Health and Human Services.

AOCS/OCAC/SEARCH

AOCS/OCAC/SEARCH is accessible via European Genome-Phenome Archive. We acknowledge their support and data, and the contribution of the study nurses, research assistants and all clinical and scientific collaborators in generation of these data. We also acknowledge their funding sources; OCAC (NIH U19CA148112), SEARCH team (Cancer Research UK C490/A16561), AOCS (U.S. Army Medical Research and Materiel Command under DAMD17-01-1-0729, The Cancer Council Victoria, Queensland Cancer Fund, The Cancer Council New South Wales, The Cancer Council South Australia, The Cancer Foundation of Western Australia, The Cancer Council Tasmania and the NHMRC (ID400413 and ID400281, as well as support from S. Boldeman, the Agar family, Ovarian Cancer Action (UK), Ovarian Cancer Australia and the Peter MacCallum Foundation).

MelaNostrum Consortium

We thank the participants of the MelaNostrum Consortium from Italy (Genoa, L'Aquila, Rome, Padua, Milan, Florence, Bergamo), Spain (Valencia, Barcelona), Greece (Athens), and Cyprus (Nicosia) who provided data and biospecimens for this study. The Consortium is partially supported by the Intramural Research Program of the Division of Cancer Epidemiology and Genetics, NCI, NIH, DHHS. Funding for the University of Genoa and Genetics of Rare Cancers, Ospedale Policlinico San Martino: Italian Ministry of Health 5×1000 per la Ricerca Corrente to Ospedale Policlinico San Martino and AIRC IG 15460. The research at the Melanoma Unit in Barcelona: The Spanish Fondo de Investigaciones Sanitarias grants PI15/00716 and PI15/00956 co-financed by FEDER "Una manera de hacer Europa"; CIBER de Enfermedades Raras of the Instituto de Salud Carlos III, Spain, co-financed by European Development Regional Fund "A way to achieve Europe" ERDF; AGAUR 2014_SGR_603 of the Catalan Government, Spain; European Commission, Contract No. LSHC-CT-2006–018702 (GenoMEL) and by the European Commission under the 7th Framework Programme, Diagnostics; "Fundació La Marató de TV3" 201331–30, Catalonia, Spain; "Fundación Científica de la Asociación Española Contra el Cáncer" GCB15152978SOEN, Spain, and CERCA Programme/Generalitat de Catalunya. Melanoma research at the Department of Dermatology, University of L'Aquila, Italy: Italian Ministry of the University and Scientific Research (PRIN-2012 grant 2012JJX494).

Q-MEGA/QTWIN

The Q-MEGA/QTWIN study was supported by the Melanoma Research Alliance, the NIH NCI (CA88363, CA83115, CA122838, CA87969, CA055075, CA100264, CA133996 and CA49449), the National Health and Medical Research Council of Australia (NHMRC) (200071, 241944, 339462, 380385, 389927,389875, 389891, 389892,389938, 443036, 442915, 442981, 496610, 496675, 496739, 552485, 552498, APP1049894), the Cancer Councils New South Wales, Victoria and Queensland, the Cancer Institute New South Wales, the Cooperative Research Centre for Discovery of Genes for Common Human Diseases (CRC), Cerylid Biosciences (Melbourne), the Australian Cancer Research Foundation, The Wellcome Trust (WT084766/Z/08/Z) and donations from Neville and Shirley Hawkins. Stuart MacGregor acknowledges fellowship support from the Australian National Health and Medical Research Council and from the Australian Research Council.

Please see the Supplementary Note for additional acknowledgments.

References

1. Karimkhani C et al. The global burden of melanoma: results from the Global Burden of Disease Study 2015. British Journal of Dermatology 177, 134–140 (2017). [PubMed: 28369739]
2. Secretan B et al. WHO International Agency for Research on Cancer Monograph Working Group A review of human carcinogens—Part E: tobacco, areca nut, alcohol, coal smoke, and salted fish. Lancet Oncol. 10, 1033–1034 (2009). [PubMed: 19891056]
3. Ford D et al. Risk of cutaneous melanoma associated with a family history of the disease. Int. J. Cancer 62, 377–381 (1995). [PubMed: 7635561]
4. Olsen CM, Carroll HJ & Whiteman DC Familial melanoma: a meta-analysis and estimates of attributable fraction. Cancer Epidemiol. Biomarkers Prev 19, 65–73 (2010). [PubMed: 20056624]
5. Olsen CM, Carroll HJ & Whiteman DC Estimating the attributable fraction for melanoma: a meta-analysis of pigmentary characteristics and freckling. Int. J. Cancer 127, 2430–2445 (2010). [PubMed: 20143394]
6. Chang YM et al. A pooled analysis of Melanocytic nevus phenotype and the risk of cutaneous melanoma at different latitudes. International Journal of Cancer (2009).
7. Olsen CM, Carroll HJ & Whiteman DC Estimating the attributable fraction for cancer: A meta-analysis of nevi and melanoma. Cancer Prev. Res 3, 233–245 (2010).

8. Bataille V et al. Nevus size and number are associated with telomere length and represent potential markers of a decreased senescence in vivo. Cancer Epidemiol. Biomarkers Prev. (2007).
9. Han J et al. A prospective study of telomere length and the risk of skin cancer. J. Invest. Dermatol (2009).
10. Green AC & Olsen CM Increased risk of melanoma in organ transplant recipients: systematic review and meta-analysis of cohort studies. Acta Derm. Venereol 95, 923–927 (2015). [PubMed: 26012553]
11. Kamb A et al. Analysis of the p16 gene (CDKN2) as a candidate for the chromosome 9p melanoma susceptibility locus. Nat. Genet 8, 23–26 (1994). [PubMed: 7987388]
12. Berwick M et al. The prevalence of CDKN2A germ-line mutations and relative risk for cutaneous malignant melanoma: an international population-based study. Cancer Epidemiol. Biomarkers Prev. 15, 1520–1525 (2006). [PubMed: 16896043]
13. Robles-Espinoza CD et al. POT1 loss-of-function variants predispose to familial melanoma. Nat. Genet (2014).
14. Shi J et al. Rare missense variants in POT1 predispose to familial cutaneous malignant melanoma. Nat. Genet 46, 482–486 (2014). [PubMed: 24686846]
15. Palmer JS et al. Melanocortin-1 receptor polymorphisms and risk of melanoma: is the association explained solely by pigmentation phenotype? Am. J. Hum. Genet 66, 176–186 (2000). [PubMed: 10631149]
16. Landi MT et al. MC1R, ASIP, and DNA repair in sporadic and familial melanoma in a mediterranean population. J. Natl. Cancer Inst (2005).
17. Brown KM et al. Common sequence variants on 20q11.22 confer melanoma susceptibility. Nat. Genet 40, 838–840 (2008). [PubMed: 18488026]
18. Bishop DT et al. Genome-wide association study identifies three loci associated with melanoma risk. Nat. Genet (2009).
19. Amos CI et al. Genome-wide association study identifies novel loci predisposing to cutaneous melanoma. Hum. Mol. Genet 20, 5012–5023 (2011). [PubMed: 21926416]
20. Barrett JH et al. Genome-wide association study identifies three new melanoma susceptibility loci. Nat. Genet (2011).
21. Macgregor S et al. Genome-wide association study identifies a new melanoma susceptibility locus at 1q21.3. Nat. Genet 43, 1114–1118 (2011). [PubMed: 21983785]
22. Iles MM et al. A variant in FTO shows association with melanoma risk not due to BMI. Nat. Genet. 45, 428–32, 432e1 (2013). [PubMed: 23455637]
23. Law MH et al. Genome-wide meta-analysis identifies five new susceptibility loci for cutaneous malignant melanoma. Nat. Genet (2015).
24. Ransohoff KJ et al. Two-stage genome-wide association study identifies a novel susceptibility locus associated with melanoma. Oncotarget 8, 17586–17592 (2017). [PubMed: 28212542]
25. Yokoyama S et al. A novel recurrent mutation in MITF predisposes to familial and sporadic melanoma. (2011).
26. Bertolotto C et al. A SUMOylation-defective MITF germline mutation predisposes to melanoma and renal carcinoma. Nature 480, 94–98 (2011). [PubMed: 22012259]
27. Duffy DL et al. Novel pleiotropic risk loci for melanoma and nevus density implicate multiple biological pathways. Nat. Commun 9, 4774 (2018). [PubMed: 30429480]
28. Zhang T et al. Cell-type-specific eQTL of primary melanocytes facilitates identification of melanoma susceptibility genes. Genome Res. 28, 1621–1635 (2018). [PubMed: 30333196]
29. Elder DE, Massi D, Willemze R & Scolyer R WHO Classification of Skin Tumours, 500 (International Agency for Research on Cancer, 2018).
30. Higgins JPT & Thompson SG Quantifying heterogeneity in a meta-analysis. Stat. Med (2002).
31. Bulik-Sullivan B et al. An atlas of genetic correlations across human diseases and traits. Nat. Genet (2015).
32. Zhang Y, Qi G, Park J-H & Chatterjee N Estimation of complex effect-size distributions using summary-level statistics from genome-wide association studies across 32 complex traits. Nat. Genet 50, 1318–1326 (2018). [PubMed: 30104760]

33. Yang J et al. Conditional and joint multiple-SNP analysis of GWAS summary statistics identifies additional variants influencing complex traits. Nat. Genet (2012).
34. Duffy DL et al. Multiple Pigmentation Gene Polymorphisms Account for a Substantial Proportion of Risk of Cutaneous Malignant Melanoma. J. Invest. Dermatol 130, 520–528 (2010). [PubMed: 19710684]
35. Duffy DL et al. IRF4 variants have age-specific effects on nevus count and predispose to melanoma. Am. J. Hum. Genet (2010).
36. Delgado DA et al. Genome-wide association study of telomere length among South Asians identifies a second RTEL1 association signal. J. Med. Genet 55, 64–71 (2018). [PubMed: 29151059]
37. Iles MM et al. The effect on melanoma risk of genes previously associated with telomere length. J. Natl. Cancer Inst 106(2014).
38. Pickrell JK et al. Detection and interpretation of shared genetic influences on 42 human traits. Nat. Genet 48, 709–717 (2016). [PubMed: 27182965]
39. Consortium, G.T. Human genomics. The Genotype-Tissue Expression (GTEx) pilot analysis: multitissue gene regulation in humans. Science 348, 648–660 (2015). [PubMed: 25954001]
40. Gamazon ER et al. A gene-based association method for mapping traits using reference transcriptome data. Nat. Genet 47, 1091–1098 (2015). [PubMed: 26258848]
41. Gusev A et al. Integrative approaches for large-scale transcriptome-wide association studies. Nat. Genet 48, 245–252 (2016). [PubMed: 26854917]
42. Finucane HK et al. Partitioning heritability by functional annotation using genome-wide association summary statistics. Nat. Genet 47, 1228–1235 (2015). [PubMed: 26414678]
43. Hormozdiari F et al. Colocalization of GWAS and eQTL Signals Detects Target Genes. Am. J. Hum. Genet 99, 1245–1260 (2016). [PubMed: 27866706]
44. Stacey SN et al. A germline variant in the TP53 polyadenylation signal confers cancer susceptibility. Nat. Genet 43, 1098–1103 (2011). [PubMed: 21946351]
45. Chahal HS et al. Genome-wide association study identifies 14 novel risk alleles associated with basal cell carcinoma. Nat. Commun 7, 12510 (2016). [PubMed: 27539887]
46. Ostrom QT et al. Sex-specific glioma genome-wide association study identifies new risk locus at 3p21.31 in females, and finds sex-differences in risk at 8q24.21. Sci. Rep 8, 7352 (2018). [PubMed: 29743610]
47. Melin BS et al. Genome-wide association study of glioma subtypes identifies specific differences in genetic susceptibility to glioblastoma and non-glioblastoma tumors. Nat. Genet 49, 789–794 (2017). [PubMed: 28346443]
48. Jin Y et al. Genome-wide association studies of autoimmune vitiligo identify 23 new risk loci and highlight key pathways and regulatory variants. Nat. Genet (2016).
49. Zhou Y, Wu H, Zhao M, Chang C & Lu Q The Bach Family of Transcription Factors: A Comprehensive Review. Clin. Rev. Allergy Immunol 50, 345–356 (2016). [PubMed: 27052415]
50. Milovic-Holm K, Krieghoff E, Jensen K, Will H & Hofmann TG FLASH links the CD95 signaling pathway to the cell nucleus and nuclear bodies. EMBO J. 26, 391–401 (2007). [PubMed: 17245429]
51. Aoude LG et al. Nonsense mutations in the shelterin complex genes ACD and TERF2IP in familial melanoma. J. Natl. Cancer Inst 107(2015).
52. Rafnar T et al. Sequence variants at the TERT-CLPTM1L locus associate with many cancer types. Nat. Genet 41, 221–227 (2009). [PubMed: 19151717]
53. Kumano K et al. Both Notch1 and Notch2 contribute to the regulation of melanocyte homeostasis. Pigment Cell Melanoma Res. 21, 70–78 (2008). [PubMed: 18353145]
54. Tang A et al. E-cadherin is the major mediator of human melanocyte adhesion to keratinocytes in vitro. J. Cell Sci 107 (Pt 4), 983–992 (1994). [PubMed: 8056851]
55. Hsu MY, Wheelock MJ, Johnson KR & Herlyn M Shifts in cadherin profiles between human normal melanocytes and melanomas. J. Investig. Dermatol. Symp. Proc 1, 188–194 (1996).
56. Study C et al. Meta-analysis of genome-wide association data identifies four new susceptibility loci for colorectal cancer. Nat. Genet 40, 1426–1435 (2008). [PubMed: 19011631]

57. Visconti A et al. Genome-wide association study in 176,678 Europeans reveals genetic loci for tanning response to sun exposure. Nat. Commun 9, 1684 (2018). [PubMed: 29739929]
58. Choi J et al. A common intronic variant of PARP1 confers melanoma risk and mediates melanocyte growth via regulation of MITF. Nat. Genet 49, 1326–1335 (2017). [PubMed: 28759004]
59. Li FP & Fraumeni JF Jr. Soft-tissue sarcomas, breast cancer, and other neoplasms. A familial syndrome? Ann. Intern. Med 71, 747–752 (1969). [PubMed: 5360287]
60. Curiel-Lewandrowski C, Speetzen LS, Cranmer L, Warneke JA & Loescher LJ Multiple primary cutaneous melanomas in Li-Fraumeni syndrome. Arch. Dermatol 147, 248–250 (2011). [PubMed: 21339461]
61. Beausejour CM Reversal of human cellular senescence: roles of the p53 and p16 pathways. The EMBO Journal 22, 4212–4222 (2003). [PubMed: 12912919]
62. Kuilman T, Michaloglou C, Mooi WJ & Peeper DS The essence of senescence. Genes Dev. 24, 2463–2479 (2010). [PubMed: 21078816]
63. Rachakonda S et al. Telomere length, telomerase reverse transcriptase promoter mutations, and melanoma risk. Genes Chromosomes Cancer (2018).
64. Choi J et al. A common intronic variant of PARP1 confers melanoma risk and mediates melanocyte growth via regulation of MITF. Nat. Genet 49(2017).
65. Derheimer FA & Kastan MB Multiple roles of ATM in monitoring and maintaining DNA integrity. FEBS Lett. 584, 3675–3681 (2010). [PubMed: 20580718]
66. Demenais F et al. A linkage study between HLA and cutaneous malignant melanoma or precursor lesions or both. J. Med. Genet 21, 429–435 (1984). [PubMed: 6595409]
67. Bale SJ et al. Hereditary malignant melanoma is not linked to the HLA complex on chromosome 6. Int. J. Cancer 36, 439–443 (1985). [PubMed: 4044054]
68. Holland EA, Beaton SC, Kefford RF & Mann GJ Linkage analysis of familial melanoma and chromosome 6 in 14 Australian kindreds. Genes Chromosomes Cancer 19, 241–249 (1997). [PubMed: 9258659]
69. Barger BO, Acton RT, Soong SJ, Roseman J & Balch C Increase of HLA-DR4 in melanoma patients from Alabama. Cancer Res. 42, 4276–4279 (1982). [PubMed: 6980704]
70. Rovini D, Sacchini V, Codazzi V, Vaglini M & Illeni MT HLA antigen frequencies in malignant melanoma patients. A second study. Tumori 70, 29–33 (1984). [PubMed: 6608815]
71. Hors J et al. HLA and Familial Malignant Melanoma. Histocompatibility Testing 1984, 407–410 (1984).
72. Lee JE, Reveille JD, Ross MI & Platsoucas CD HLA-DQB1* 0301 association with increased cutaneous melanoma risk. International journal of cancer 59, 510–513 (1994). [PubMed: 7960221]
73. Muto M et al. HLA class I polymorphism and the susceptibility to malignant melanoma. Tissue Antigens 47, 447–449 (1996). [PubMed: 8795150]
74. Kageshita T et al. Molecular genetic analysis of HLA class II alleles in Japanese patients with melanoma. Tissue Antigens 49, 466–470 (1997). [PubMed: 9174138]
75. Bateman AC, Turner SJ, Theaker JM & Howell WM HLA-DQB1*0303 and *0301 alleles influence susceptibility to and prognosis in cutaneous malignant melanoma in the British Caucasian population. Tissue Antigens 52, 67–73 (1998). [PubMed: 9714476]
76. Lombardi ML et al. Molecular analysis of HLA DRB1 and DQB1 polymorphism in Italian melanoma patients. J. Immunother 21, 435–439 (1998). [PubMed: 9807738]
77. Luongo V et al. HLA allele frequency and clinical outcome in Italian patients with cutaneous melanoma. Tissue Antigens 64, 84–87 (2004). [PubMed: 15191529]
78. Campillo JA et al. HLA class I and class II frequencies in patients with cutaneous malignant melanoma from southeastern Spain: the role of HLA-C in disease prognosis. Immunogenetics 57, 926–933 (2006). [PubMed: 16365741]
79. Planelles D et al. HLA class II polymorphisms in Spanish melanoma patients: homozygosity for HLA-DQA1 locus can be a potential melanoma risk factor. Br. J. Dermatol 154, 261–266 (2006). [PubMed: 16433795]
80. Jin Y et al. Genome-wide association analyses identify 13 new susceptibility loci for generalized vitiligo. Nat. Genet 44, 676–680 (2012). [PubMed: 22561518]

81. Curran K et al. Interplay between Foxd3 and Mitf regulates cell fate plasticity in the zebrafish neural crest. Dev. Biol 344, 107–118 (2010). [PubMed: 20460180]
82. Thomas AJ & Erickson CA FOXD3 regulates the lineage switch between neural crest-derived glial cells and pigment cells by repressing MITF through a non-canonical mechanism. Development 136, 1849–1858 (2009). [PubMed: 19403660]
83. Schouwey K, Larue L, Radtke F, Delmas V & Beermann F Transgenic expression of Notch in melanocytes demonstrates RBP-Jkappa-dependent signaling. Pigment Cell Melanoma Res. 23, 134–136 (2010). [PubMed: 19895548]
84. Zabierowski SE et al. Direct reprogramming of melanocytes to neural crest stem-like cells by one defined factor. Stem Cells 29, 1752–1762 (2011). [PubMed: 21948558]
85. Falchi M et al. Genome-wide association study identifies variants at 9p21 and 22q13 associated with development of cutaneous nevi. Nat. Genet 41, 915–919 (2009). [PubMed: 19578365]
86. Garraway LA et al. Integrative genomic analyses identify MITF as a lineage survival oncogene amplified in malignant melanoma. Nature (2005).
87. Abel EV & Aplin AE FOXD3 is a mutant B-RAF-regulated inhibitor of G(1)-S progression in melanoma cells. Cancer Res. 70, 2891–2900 (2010). [PubMed: 20332228]
88. Weiss MB, Abel EV, Dadpey N & Aplin AE FOXD3 modulates migration through direct transcriptional repression of TWIST1 in melanoma. Mol. Cancer Res 12, 1314–1323 (2014). [PubMed: 25061102]
89. Golan T et al. Interactions of Melanoma Cells with Distal Keratinocytes Trigger Metastasis via Notch Signaling Inhibition of MITF. Mol. Cell (2015).
90. Cronin JC et al. SOX10 ablation arrests cell cycle, induces senescence, and suppresses melanomagenesis. Cancer Res. (2013).
91. Guilford P et al. E-cadherin germline mutations in familial gastric cancer. Nature 392, 402–405 (1998). [PubMed: 9537325]
92. Hansford S et al. Hereditary Diffuse Gastric Cancer Syndrome: CDH1 Mutations and Beyond. JAMA Oncol 1, 23–32 (2015). [PubMed: 26182300]
93. Kim HC et al. The E-cadherin gene (CDH1) variants T340A and L599V in gastric and colorectal cancer patients in Korea. Gut 47, 262–267 (2000). [PubMed: 10896919]
94. Wagner RY et al. Altered E-Cadherin Levels and Distribution in Melanocytes Precede Clinical Manifestations of Vitiligo. J. Invest. Dermatol 135, 1810–1819 (2015). [PubMed: 25634357]
95. Padmanaban V et al. E-cadherin is required for metastasis in multiple models of breast cancer. Nature 573, 439–444 (2019). [PubMed: 31485072]

Methods References

96. Purcell S et al. PLINK: a tool set for whole-genome association and population-based linkage analyses. Am. J. Hum. Genet 81, 559–575 (2007). [PubMed: 17701901]
97. Chang CC et al. Second-generation PLINK: rising to the challenge of larger and richer datasets. Gigascience 4, 7 (2015). [PubMed: 25722852]
98. Das S et al. Next-generation genotype imputation service and methods. Nat. Genet 48, 1284–1287 (2016). [PubMed: 27571263]
99. DerSimonian R & Laird N Meta-analysis in clinical trials. Control. Clin. Trials 7, 177–188 (1986). [PubMed: 3802833]
100. Machiela MJ & Chanock SJ LDassoc: an online tool for interactively exploring genome-wide association study results and prioritizing variants for functional investigation. Bioinformatics 34, 887–889 (2018). [PubMed: 28968746]
101. Willer CJ, Li Y & Abecasis GR METAL: Fast and efficient meta-analysis of genomewide association scans. Bioinformatics (2010).
102. Watanabe K, Taskesen E, Van Bochoven A & Posthuma D Functional mapping and annotation of genetic associations with FUMA. Nat. Commun (2017).
103. Bulik-Sullivan BK et al. LD Score regression distinguishes confounding from polygenicity in genome-wide association studies. Nat. Genet 47, 291–295 (2015). [PubMed: 25642630]

104. Australian Institute of, H. & Welfare. Cancer in Australia: Actual incidence data from 1982 to 2013 and mortality data from 1982 to 2014 with projections to 2017. Asia Pac. J. Clin. Oncol 14, 5–15 (2018).

105. DeLuca DS et al. RNA-SeQC: RNA-seq metrics for quality control and process optimization. Bioinformatics 28, 1530–1532 (2012). [PubMed: 22539670]

106. Finucane HK et al. Heritability enrichment of specifically expressed genes identifies disease-relevant tissues and cell types. Nat. Genet 50, 621–629 (2018). [PubMed: 29632380]

107. McCarthy S et al. A reference panel of 64,976 haplotypes for genotype imputation. Nat. Genet 48, 1279–1283 (2016). [PubMed: 27548312]

108. MacGregor S et al. Two novel loci for melanoma susceptibility on chromosome bands 1q42.12 and 1q21.3. Nat. Genet (2011).

109. Peña-Chilet M et al. Genetic variants in PARP1 (rs3219090) and IRF4 (rs12203592) genes associated with melanoma susceptibility in a Spanish population. BMC Cancer 13(2013).

110. Law MH et al. Meta-analysis combining new and existing data sets confirms that the TERT-CLPTM1L locus influences melanoma risk. J. Invest. Dermatol 132, 485–487 (2012). [PubMed: 21993562]

111. Antonopoulou K et al. Updated field synopsis and systematic meta-analyses of genetic association studies in cutaneous melanoma: the MelGene database. J. Invest. Dermatol 135, 1074–1079 (2015). [PubMed: 25407435]

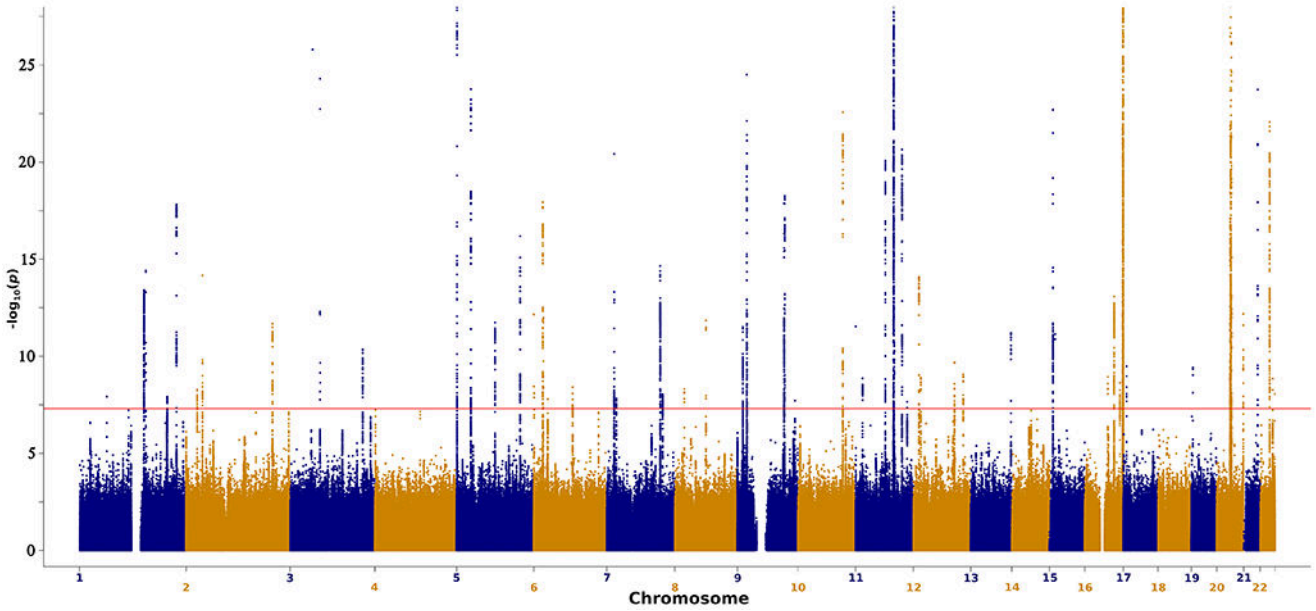

Figure 1. Manhattan plot for the total cutaneous melanoma meta-analysis.

$-\log_{10}$ of two-sided P-values for SNPs derived from a fixed-effects inverse variance weighted meta-analysis of logistic regression GWAS (Y-axis) plotted against SNP chromosome positions for the total meta-analysis (36,760 melanoma cases and 375,188 controls; for full details of analysis and covariates included see the Online Methods). The y-axis is limited to $-\log_{10}(1\times10^{-25})$ to truncate strong signals at loci such as *MC1R* and *ASIP*. The full plot is displayed in Extended Data Figure 2. To account for multiple testing, SNPs with a P-value less than 5×10^{-8} are deemed significant.

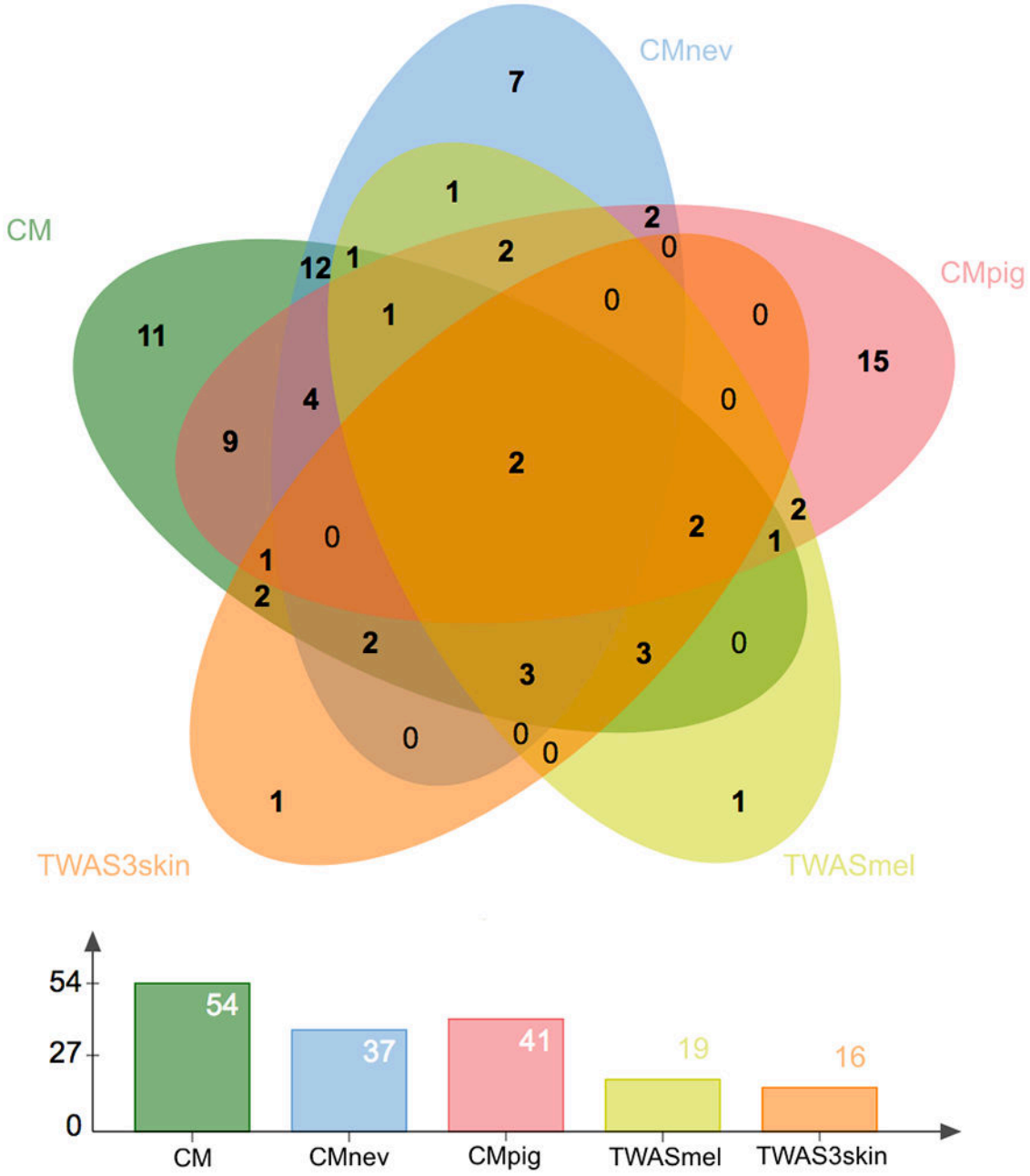

Figure 2. Overlap of loci identified by primary and secondary analyses.

Loci identified in the **total** cutaneous melanoma meta-analysis (CM, green, Supplementary Table 3), the pleiotropic analysis with nevus count (CMnev, blue, Supplementary Table 9) and hair color (CMpig, red, Supplementary Table 10), melanocyte TWAS (TWASmel, yellow, Supplementary Table 10), and TWAS using the expression of three skin tissues (TWAS3skin, orange, Supplementary Table 12).